Published by :
http://www.ijert.org

International Journal of Engineering Research & Technology (IJERT)
ISSN: 2278-0181
Volume 13, Issue 01 January 2024

Calculation of Basic Elements of A Radial-type Centrifugal Pump.

A comparative study for blade shape configurations and blade curvature of Impeller and Spiral Shell.

J.C.Statharas (corresponding author)
Professor, General Department of Engineering Science ,
National & Kapodistrian University of Athens , 34400
Psachna Evias, Chalkis Greece

Vasileios N Vlachakis
Research Associate,Engineering Mechanics
, Virginia Polytechnic Institute & State University,
Blacksburg, VA 24060

P.S.Filiousis
Mechanical Engineer, External Research Fellow

N.W.Vlachakis
Professor, Research Fellow

***Abstract*—A contribution on centrifugal pump characteristics prediction is presented using relations based on performance maps of known pumps developed by some researchers. The introduced modelling equations based on the blade shape configurations, approximate satisfactorily the geometry of industrial centrifugal pumps elements (vane, shell, meridional section etc.). Also a fast calculation of the distribution of the blade angles in the entire blade curvature is developed using smart algorithms eliminating the need of time-consuming tables of classical methodologies.**

***Keywords*—**Centrifugal pump , Volute casing , algorithms for design, flow characteristics, Velocity triangles, blade shape configurations, Blade Profiles, wrap angle, diagram of the impeller.

I. INTRODUCTION

Pumps are one of the most interesting devices in mechanical engineering and constitute the heart of a large sector of industrial and public networks, piping networks etc. There is a wide range of pump types quite different from each other in terms of operating principle, structure and the applications they cover. A basic category, however, is centrifugal pumps of radial type.

Centrifugal pumps use the centrifugal force created by a rotating disk on which there are vanes of a special shape and which is known as an impeller or impeller.Fluid flow in centrifugal pumps is created by the centrifugal kinetic energy produced by the rotary motion of the impeller. The aspirated liquid reaches the suction opening and is swept into rotation driven by the vanes. The rotary motion of the impeller imparts rotation to the liquid mass which is driven by the vanes imparting centrifugal force to the liquid. The liquid is forced to flow along the vanes and ejected from the impeller. As soon as the liquid escapes from the impeller, it is collected in an internal space of the pump, which has a spiral shape with an ever-increasing cross-section and finally leaves the pump outlet.

Although there is a wide range of centrifugal pumps there are common comparative advantages of all types of centrifugal pumps over other types of pumps. These are their laminar and smooth operation but mainly their operational flexibility in the sense of the possibility of choosing the desired operating range according to the H-Q (Head-Discharge) diagram. At the same time, centrifugal pumps generally require little space compared to other types of pumps for the same pressure gauge or flow rate. Centrifugal pumps, however, have the ability to offer pump types with very high outputs that other types of pumps cannot achieve and for this reason they are usually preferred in high output lines.

(This work is licensed under a Creative Commons Attribution 4.0 International License.)

International Journal of Engineering Research & Technology (IJERT)
ISSN: 2278-0181
Volume 13, Issue 01 January 2024

The basic parts of centrifugal pumps are the impeller, the volute and the inlet and outlet ducts (Fig.1.1)

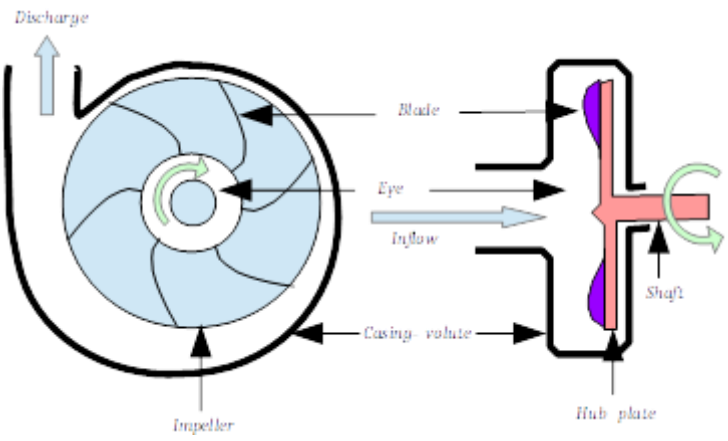

Fig. 1.1. Main parts of a radial-type centrifugal pump

For the design of individual parts of centrifugal pumps, one can find in the literature several methods from the simplest to the most complex (e.g. [1],[2],[3]). In this paper we do not intend to review all these methods but to present a relatively simple but at the same time detailed, precise and practical method for the design of the various parts of a centrifugal pump. This method can be used to design any centrifugal pump.

In chapter II, the proposed design method is presented with its simultaneous application to the design of a pump for the purposes of demonstration of the method. The main purpose of this chapter is the detailed and precise design and drawing of the meridional section of the pump, its impeller as well as the configuration of the inlet and outlet sections and the spiral shell.

In chapter III, some empirical relations are proposed for the prediction of basic performance characteristics of a pump. The predictions of these relations are compared with the experimental ones. The comparison concerns the pressure head, the performance and the $NPSH_R$ of some pumps from different manufacturers. This comparison is necessary to confirm that the proposed model actually achieves its intended purpose, i.e. for validation purposes.

I. MODELLING PUMP GEOMETRY

In what follows, the design method of a centrifugal pump will be presented. At the same time, for demonstration purposes, the method will be applied to the design of a pump with given characteristics. The characteristics of the pump to be designed are taken from ([1],[2],[3]) and are shown in Table I.

TABLE I. characteristics values used for the centrifugal pump to be designed.

manometric Head H (m)	50
critical cavitation height H_{cr} (m)	3
Flow rate Q(m^3/h)	300
Blade angle at outlet β_2 (degrees)	18
g (m/(s^2))	9,81
Water density, ρ (Kg/m^3)	1.000
Water kinematic viscosity ν*(m^2/s)	0,000001
Water temperature θ(^{0}C)	15
impeller's number of blades z= β_2/3	6

(This work is licensed under a Creative Commons Attribution 4.0 International License.)

International Journal of Engineering Research & Technology (IJERT)
ISSN: 2278-0181
Volume 13, Issue 01 January 2024

A. Centrifugal Pump Structure Design.

The procedure for designing the centrifugal pump structure is according to ([5],[7],[9],[15]). By knowing the head pump H and the Thomas' cavitation parameter σ=1,5, we can calculate the critical cavitation parameter σ_{cr}:

$$\sigma_{cr} = \frac{\sigma}{H} \rightarrow \sigma_{cr} = \frac{1,5}{50} = 0.03 \tag{2.1}$$

Using Bohl's formula, we calculate the rotation specific speed n_q:

$$\sigma_{cr} = 0.077 \cdot n_q^{\frac{4}{3}} \rightarrow n_q = \frac{(\sigma_{cr})^{\frac{3}{4}}}{0.077} \rightarrow$$

$$\rightarrow n_q = \frac{(0,03)^{\frac{3}{4}}}{0.077} \rightarrow n_q = 29.22\, rpm \tag{2.2}$$

By using the formula of specific speed, the pump rotational speed n is obtained:

$$\eta_q = n \cdot \frac{(Q/3600)^{0,5}}{H^{\frac{3}{4}}} \rightarrow n = \frac{\eta_q \cdot H^{\frac{3}{4}}}{(Q/3600)^{0,5}} \rightarrow$$

$$\rightarrow n = \frac{29,22 \cdot 50^{\frac{3}{4}}}{(300/3600)^{0,5}} \rightarrow n = 1903\, rpm \tag{2.3}$$

It is known that the parameter ψ is defined by the relationship:

$$\psi = \frac{2}{n_q^{0.2}} = \frac{2}{29,22^{0.2}} = 1.01 \tag{2.4}$$

The specific pump work Y is:

$$Y = g \cdot H = 9.81 \cdot 50 = 490.5\, J/kg \tag{2.5}$$

Therefore the impeller outlet diameter D_2 is:

$$D_2 = 0.45 \cdot \frac{(Y/\psi)^{0.5}}{(n/60)} \rightarrow$$

$$D_2 = 0.45 \cdot \frac{(490.5/1.01)^{0.5}}{(1903/60)} = 0.31\, m \tag{2.6}$$

The impeller inlet diameter is selected to be:

$$D_1 = 0.48 \cdot D_2 = 0.15\, m \tag{2.7}$$

Then the outlet tangential velocity u_2 is:

$$u_2 = 3.14 \cdot D_2 \cdot (n/60) \rightarrow$$

$$u_2 = 3.14 \cdot 0.31 \cdot (1903/60) = 31\, m/s \tag{2.8}$$

and the inlet tangential velocity u_1 is:

$$u_1 = 3.14 \cdot D_1 \cdot (n/60) \rightarrow$$

$$u_1 = 3.14 \cdot 0.15 \cdot (1903/60) = 14.8\, m/s \tag{2.9}$$

The special speed coefficients k_{m1} and k_{m2} are:

$$k_{m1} = 0.07 + 0.002 \cdot n_q \rightarrow$$

$$k_{m1} = 0.07 + 0.002 \cdot 29.22 = 0.12 \tag{2.10}$$

and

$$k_{m2} = 0.063 + 0.0017 \cdot n_q \rightarrow$$

$$k_{m2} = 0.063 + 0.0017 \cdot 29.22 = 0.11 \tag{2.11}$$

(This work is licensed under a Creative Commons Attribution 4.0 International License.)

International Journal of Engineering Research & Technology (IJERT)
ISSN: 2278-0181
Volume 13, Issue 01 January 2024

The variation of k_{m1} and k_{m2} with n_q is shown in Fig.2.1 and Fig.2.2 respectively.

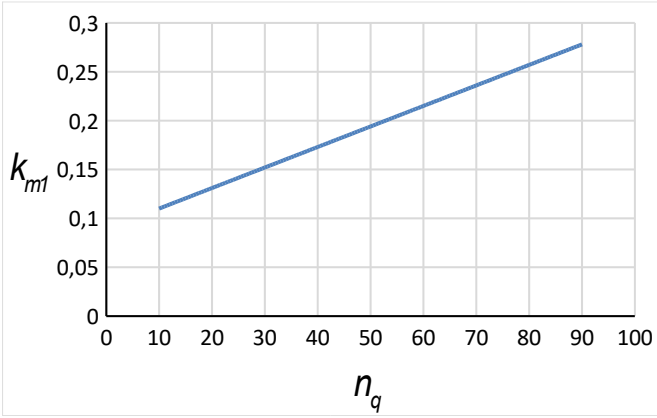

Fig. 2. 1, Inlet flow velocity coefficient k_{m1}

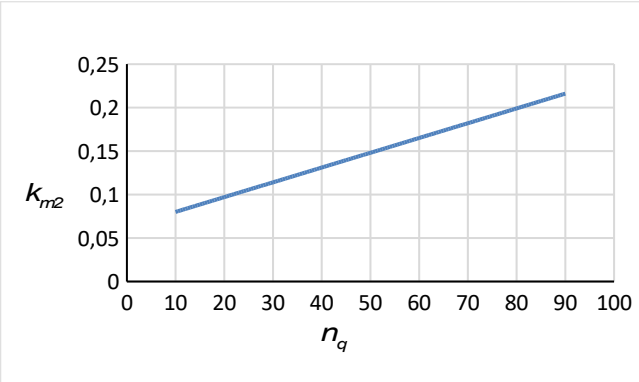

Fig.2.2. Outlet flow velocity coefficient k_{m2}.

The meridional flow velocity at the impeller inlet is:

$$V_{1m} = c_{m1} = k_{m1} \cdot (2 \cdot Y)^{0.5} \rightarrow$$

$$V_{1m} = c_{m1} = 0.12 \cdot (2 \cdot 490.5)^{0.5} = 4.02\, m/s \qquad (2.12)$$

The meridional flow velocity at the impeller outlet is.

$$V_{2m} = c_{m2} = k_{m2} \cdot (2 \cdot Y)^{0.5} \rightarrow$$

$$V_{2m} = c_{m2} = 0.11 \cdot (2 \cdot 490.5)^{0.5} = 3.52\, m/s \qquad (2.13)$$

A. Calculation of blades' widths

The flow rate factors k_1 and k_2 that are used to determine the blades' widths, are:

$$k_1 = \frac{\pi \cdot D_1}{\pi \cdot D_1 - z \cdot \dfrac{s_1}{\sin(\pi \cdot \dfrac{\beta_1}{180})}} \rightarrow$$

$$k_1 = \frac{3.14 \cdot 0.15}{3.14 \cdot 0.15 - 6 \cdot \dfrac{0.0099}{\sin(3.14 \cdot \dfrac{15}{180})}} = 1.53 \qquad (2.14)$$

(This work is licensed under a Creative Commons Attribution 4.0 International License.)

International Journal of Engineering Research & Technology (IJERT)
ISSN: 2278-0181
Volume 13, Issue 01 January 2024

where: $\beta_1=15^0$ and $s_1=D_1/15=0.15/15=0.0099\ m$, is the blade thickness at the inlet,

and

$$k_2=\frac{\pi\cdot D_2}{\pi\cdot D_2-z\cdot\frac{s_1}{\sin(\pi\cdot\frac{\beta_2}{180})}}\rightarrow$$

$$k_2=\frac{3.14\cdot 0.31}{3.14\cdot 0.31-6\cdot\frac{0.0062}{\sin(3.14\cdot\frac{18}{180})}}=1.1 \qquad (2.15)$$

where: $\beta_2=18^0$ and $s_2=D_2/50=0.31/50=0.0062\ m$, is the blade thickness at the exit.
The blade's width in the impeller inlet is:

$$b_1=\frac{k_1\cdot Q}{c_{m1}\cdot 3.14\cdot D_1}\rightarrow \qquad b_1=\frac{1.53\cdot 300/3600}{4.02\cdot 3.14\cdot 0.15}=0.044\,m \qquad (2.16)$$

where:

$$Q=c_{m1}\cdot A_1$$

and A_1 is the section area at the impeller inlet.
The blade's width in the impeller outlet is:

$$b_2=\frac{k_2\cdot Q}{c_{m2}\cdot 3.14\cdot D_2}\rightarrow \qquad b_2=\frac{1.1\cdot 300/3600}{3.52\cdot 3.14\cdot 0.31}=0.024\,m \qquad (2.17)$$

where:

$$Q=c_{m2}\cdot A_2$$

and A_2 is the section area at the impeller outlet.

B. Calculation of velocity diagrams.

Now we can calculate the other speeds in order to form the inlet and outlet velocity diagrams.
The inlet velocity c_o at the suction cross-section is:

$$c_o=0.02\cdot n_q^{0.66}\cdot(2\cdot Y)^{0.5}\rightarrow$$
$$c_o=0.02\cdot 29.22^{0.66}\cdot(2\cdot 490.5)^{0.5}\rightarrow$$
$$c_o=5.81\,m/s=c_1 \qquad (2.18)$$

So the inlet relative velocity w_1 is:

$$w_1=(u_1^2+c_o^2)^{0,5}\rightarrow$$
$$w_1=(14.8^2+5.81^2)^{0,5}=15.92\,m/s \qquad (2.19)$$

The outlet relative velocity w_2 can be calculated as follows:

$$w_{2u}=\frac{c_{m2}}{\tan(\frac{\beta_2\cdot\pi}{180})}\rightarrow$$

$$w_{2u}=\frac{3.52}{\tan(\frac{18\cdot 3.14}{180})}=12.51\,m/s \qquad (2.20)$$

and: $w_{m2}=c_{m2}=3.52$ m/s , so:

$$w_2=(w_{2u}^2+w_{m2}^2)^{0.5}\rightarrow$$
$$w_2=(12.51^2+3.52^2)^{0.5}=13\,m/s \qquad (2.21)$$

We can now calculate the absolute velocities:

(This work is licensed under a Creative Commons Attribution 4.0 International License.)

International Journal of Engineering Research & Technology (IJERT)
ISSN: 2278-0181
Volume 13, Issue 01 January 2024

$c_{u2}=u_2-w_{2u}=31-12.51=18.52$ m/s (2.22)

or

$$V_{1u}= V_{1m}\cot(a_1)= c_{u2}= c_{m1}\cot(a_1) \quad (2.23)$$

$$V_{2u}= c_{u2}= u_2- c_{m2}\cot(\beta_2) \quad (2.24)$$

$$c_2=(c_{u2}^2+c_{m2}^2)^{0.5}=(18.52^2+3.52^2)^{0.5}=18.85 \quad (2.25)$$

Fig.2.3. Shows the velocity triangles at impeller inlet and Fig.2.4 for the outlet. A schematic reprsentation of the velocity triangles at impeller is shown in Fig.2.5.

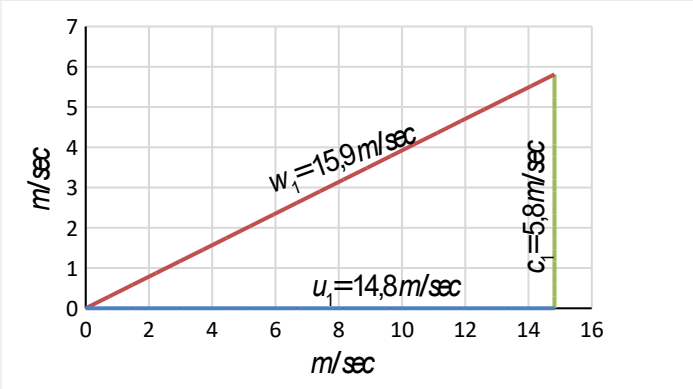

Fig.2.3. Inlet Velocity Diagram

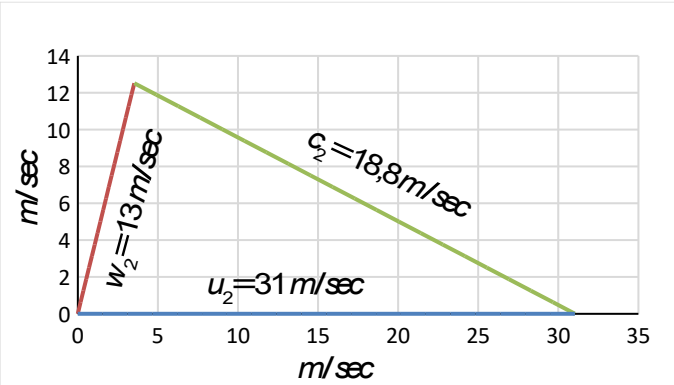

Fig.2.4. Outlet Velocity Diagram

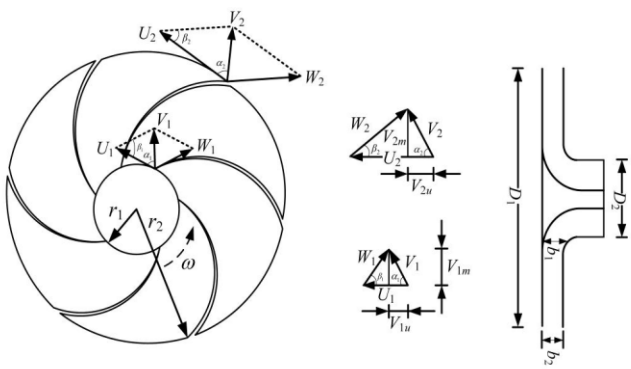

Fig.2.5. The velocity triangles at the impeller of a centrifugal pump, [9]

(This work is licensed under a Creative Commons Attribution 4.0 International License.)

International Journal of Engineering Research & Technology (IJERT)
ISSN: 2278-0181
Volume 13, Issue 01 January 2024

C. Calculation of shaft diameter

We have first to calculate pump's efficiency. The calculation of the performance efficiencies, is derived according to ([5],[8]) :

Mechanical efficiency

$$n_m = \frac{1}{1+\frac{0.287}{n_q^{0.66}}} = \frac{1}{1+\frac{0.287}{29.22^{0.66}}} = 0.968 \quad (2.26)$$

or

$$n_m = \frac{1}{1+\frac{15.05}{n_q^{1.8}}} = \frac{1}{1+\frac{15.05}{29.22^{1.8}}} = 0.966 \quad (2.27)$$

volumetric efficiency

$$\eta_q = \frac{1}{1+\frac{0.46}{n_q^{0.84}}} = \frac{1}{1+\frac{0.46}{29.22^{0.84}}} = 0.97 \quad (2.28)$$

while the hydraulic efficiency is:

$$\eta_h = \frac{1-0.071}{\frac{n_q}{3600}^{0.25}} = \frac{1-0.071}{\frac{29.22}{3600}^{0.25}} = 0.867 \quad (2.29)$$

The overall Pump efficiency is: $\eta_t=\eta_q\cdot\eta_m\cdot\eta_h=0.8$. (2.30)

The water power N is determined from the relationship:

$$N = \frac{\rho\cdot Y\cdot Q}{\eta_t} \rightarrow$$

$$N = \frac{1000\cdot 490.5\cdot (300/3600)}{0.8} = 51093\, Watt \quad (2.31)$$

The methodology for designing the blade geometry and the meridian geometry follows Ref.[6]. According to [6] the torsional moment is estimated to be:

$$M_d = \frac{N}{2\pi\cdot n} \rightarrow$$

$$M_d = \frac{51093}{6.28\cdot (1903.3/60)} = 256{,}47\, N\cdot m \quad (2.32)$$

The shaft diameter is:

$$d_w = 1000\frac{\cdot M_d}{(0.2\cdot\tau)^{0.33}} \rightarrow$$

$$d_w = 1000\frac{\cdot 256{,}47}{(0.2\cdot 50)^{0.33}} = 29.4\, mm \quad (2.33)$$

where the volute suction diameter of impeller D_s is:
$D_s=0.42\cdot D_2=0.13m$

(This work is licensed under a Creative Commons Attribution 4.0 International License.)

International Journal of Engineering Research & Technology (IJERT)
ISSN: 2278-0181
Volume 13, Issue 01 January 2024

D. The camber surface of the blade meridional profile of impeller.

The meridian section of the pump is calculated for its curved parts (internal and external) from the dimensions of the blades diameters and blades thicknesses for various selected functions shown in Table II.

TABLE II. Walls coordinates and boundary conditions for the camber surface of the blade meridional profile of impeller.

A		B		D		C	
x_a	y_a	x_b	y_b	x_d	y_d	x_c	y_c
0,000795	0,000795	0	0,05	0,11	0,19885	0,09	0,19885
wall function 1 (ξ=3)				wall function 2 (ξ=2)		wall algorithms $y=a\cdot\exp(c\cdot x^{\xi})$	
c	a			c"	a"		
1988,433	0,052496			3998,65	0,00079		
x	y			x	y		
0,000795	0,052496			0,00079	0,00079		
0,010429	0,052614			0,01307	0,00080		
0,020062	0,053345			0,02536	0,00084		
0,029695	0,055301			0,03764	0,00098		
0,039328	0,059245			0,04993	0,00130		
0,048961	0,066295			0,06221	0,00208		
0,058594	0,078316			0,074	0,00415		
0,068228	0,098717			0,086	0,01		
0,077861	0,134196			0,099	0,038		
0,087	0,19885			0,11	0,19885		

The resulting meridian section of the pump is shown in Fig.2.6.

(This work is licensed under a Creative Commons Attribution 4.0 International License.)

International Journal of Engineering Research & Technology (IJERT)
ISSN: 2278-0181
Volume 13, Issue 01 January 2024

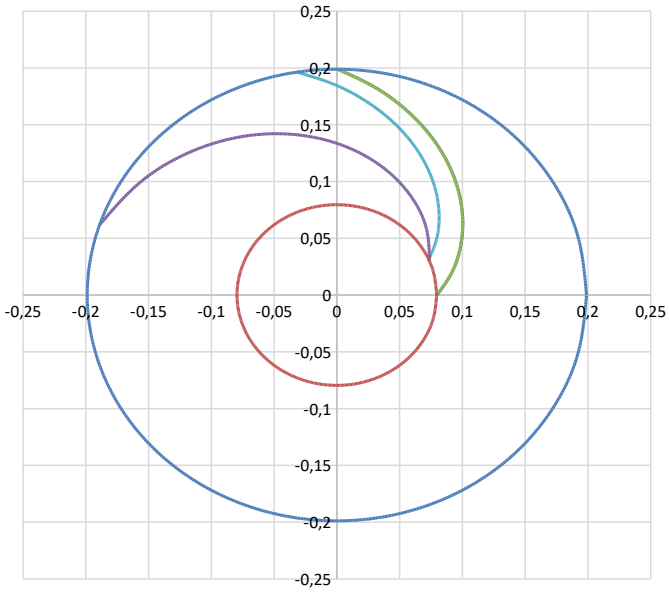

Fig.2.6. The Meridian section of the pump

For the meridian section of the impeller we use the following wall algorithms:

$$y = a \exp(c\, x^{\xi}) \qquad (2.34)$$

obtaining the x and y values shown in Table III.

TABLE III. IMPELLER'S MERIDIAN SECTION COORDINATES

b_1		b_2	
x_{b1}	y_{b1}	x_{b2}	y_{b2}
0,000795	0,000795	0,087494	0,19885
0,000795	0,051701	0,111356	0,19885

The resulting meridian section of the impeller is shown in

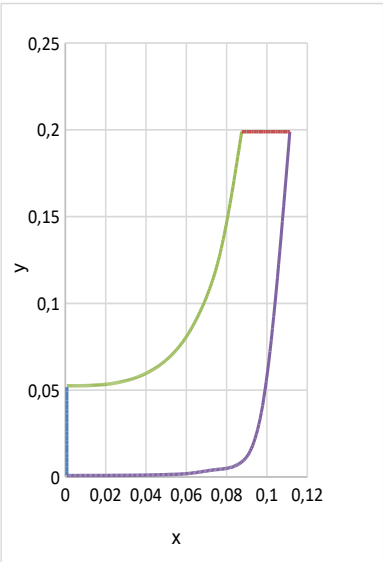

Fig.2.7. Meridional profile of impeller

(This work is licensed under a Creative Commons Attribution 4.0 International License.)

International Journal of Engineering Research & Technology (IJERT)
ISSN: 2278-0181
Volume 13, Issue 01 January 2024

E. Design of the blades on the impeller

The design of the impeller's blades follows the procedure described in [4]. The obtained geometrical results are shown in Table IV.

TABLE IV. Blade shape configuration using Sigloch methodology.

points	r_x	Δr_x	b_x	w_x	t_x	β_x	h_x	h_x»	h»»	b_x»»»	φ
	1	mm	mm	m/sec							
1	0,07	0,0091	44,3	15,9	0,07	15,7	47,6	0	0	44,3	0
2	0,08	0,0091	42	15,4	0,08	15,9	41,8	0,41	0,41	40	23,5
3	0,09	0,0091	39,8	14,9	0,09	16,2	37,1	0,36	0,77	36,6	44,2
4	0,1	0,0091	37,6	14,5	0,1	16,4	33,1	0,32	1,09	33,8	62,7
5	0,11	0,0091	35,3	14	0,11	16,7	29,8	0,28	1,38	31,5	79,3
6	0,12	0,0091	33,1	13,5	0,12	17	27	0,26	1,64	29,5	94,2
7	0,12	0,0091	30,8	13	0,13	17,4	24,6	0,23	1,88	27,9	107,8
8	0,13	0,0091	28,6	12,6	0,14	17,7	22,5	0,21	2,09	26,4	120,2
9	0,14	0,0091	26,3	12,1	0,15	18,1	20,6	0,19	2,29	25,1	131,5
10	0,15	-0,15	24,1	11,6	0,16	18,5	18,9	0,18	2,47	24	141,9

With the first blade showing the calculation arrangement shown in Table V.

TABLE V. First blade calculation arrangement

x_a	y_a	φ_{o1}	φ_1	r_1
0,0744	0	0°	0°	0,0744
0,0722	0,0314	Wrap angle	23,514°	0,0787
0,0601	0,0585	141,99°	44,256°	0,0839
0,0413	0,0799		62,728°	0,0899
0,0181	0,0954		79,307°	0,0971
-0,008	0,1052		94,278°	0,1055
-0,035	0,1098		107,87°	0,1153
-0,064	0,1097		120,25°	0,127
-0,093	0,1053		131,59°	0,1407
-0,124	0,0968		141,99°	0,1569

The geometry of the pump we selected to design, also determines the wrap angle φ_w as follows [12] :

$$\varphi_w = (\beta_2 - \beta_1)\frac{\cdot \ln(\frac{r_2}{r_1})}{[\frac{\ln(\cos\beta_1)}{\cos\beta_2}]} = (\beta_2 - \beta_1)\frac{\cdot \ln(\frac{D_2}{D_1})}{[\frac{\ln(\cos\beta_1)}{\cos\beta_2}]} \rightarrow$$

$$\rightarrow \varphi_w = (18 - 15)\frac{\cdot \ln(\frac{0,31}{0,15})}{[\frac{\ln(\cos 15)}{\cos 18}]} = 141^0 \qquad (2.35)$$

For a fast track calculation the distribution of the blade curvature can also be proposed here with the algorithms:

(This work is licensed under a Creative Commons Attribution 4.0 International License.)

International Journal of Engineering Research & Technology (IJERT)
ISSN: 2278-0181
Volume 13, Issue 01 January 2024

$$y = a \ln(r_i) + c \qquad (2.36)$$

where:

$$a = \frac{0.8 \cdot \varphi_w}{\ln(\frac{r_i}{r_2})} \quad \text{and} \quad c = \varphi_w \cdot [1 - \frac{0.8 \ln(r_i)}{\ln(\frac{r_i}{r_2})}] \qquad \text{(I)}$$

$$\varphi = \varphi_\varepsilon \frac{\frac{r}{r_1} - (\frac{r}{r_1})\xi}{\frac{r_2}{r_1} - (\frac{r_2}{r_1})\xi} \qquad (2.37)$$

where $-2 < \xi < 2$ (II)

The parameter ξ can independently determine the blade shape y or the thickness of y. The two methods (I) and (II) are almost identical.
These shape forms are preferred because laboratory tests have shown that the blades are safe against impact or friction**.** The results obtained using these shape forms are shown in Table VI. The corresponding blade shape is shown in Fig.2.8.

TABLE VI. FAST TRACK CALCULATION OF THE BLADE CURVATURE

x_a	y_a	φ_{o1}	φ_1	r_1
0,0795	0	0°	0°	0,0795
0,0818	0,0438	Wrap angle	28,2°	0,0928
0,071	0,0787	141	47,963°	0,1061
0,0497	0,1084		65,396°	0,1193
0,0209	0,1309		80,989°	0,1326
-0,013	0,1453		95,096°	0,1458
-0,049	0,1514		107,97°	0,1591
-0,086	0,1496		119,82°	0,1723
-0,121	0,1407		130,79°	0,1856
-0,154	0,1253		141°	0,1988

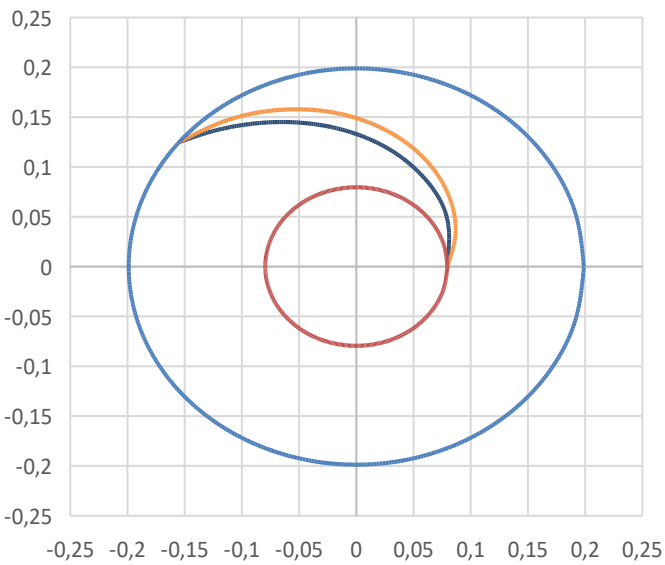

Fig.2.8. The blade shape can also be specified with other functions

(This work is licensed under a Creative Commons Attribution 4.0 International License.)

International Journal of Engineering Research & Technology (IJERT)
ISSN: 2278-0181
Volume 13, Issue 01 January 2024

Some proposed functions according to ([13],[14]) for the blade shape are:

$$\varphi = \frac{\varphi_{\varepsilon} \cdot \ln\left(\frac{r}{r_2}\right)}{\ln\left(\frac{r_2}{r_1}\right)} \quad (2.38)$$

$\varphi = \alpha \cdot \ln(r) + c$ (2.39)

and $\varphi = \alpha \cdot J1((r/r_1)-1)$ (2.40)

with the boundary conditions:

$r=r_1$ for $\varphi=0$

$r=r_2$ for $\varphi=\varphi_w$

The results are shown in Table VII.

TABLE VII. BLADE SHAPE CONFIGURATION FOR DIFFERENT ALGORITHMS

φ_i Sigloch	φ_i ln	φ_i alnr+c	φ_i besselJ1
0	0	0	0
25,79029144	23,74	28,223	21,01241572
47,44841549	44,304	48,002	41,58808522
66,05705779	62,444	65,448	61,30034879
82,32884465	78,67	81,054	79,74247507
96,75664773	93,348	95,172	96,53701991
109,6948682	106,75	108,06	111,3444756
121,4064634	119,07	119,92	123,8710021
132,0916559	130,49	130,89	133,8750534
141,9062476	141,11	141,11	141,1727423

Fig.2.9 shows the blade profile and the impeller morphology for 6 blades with blade curvature according to Sigloch methodology.

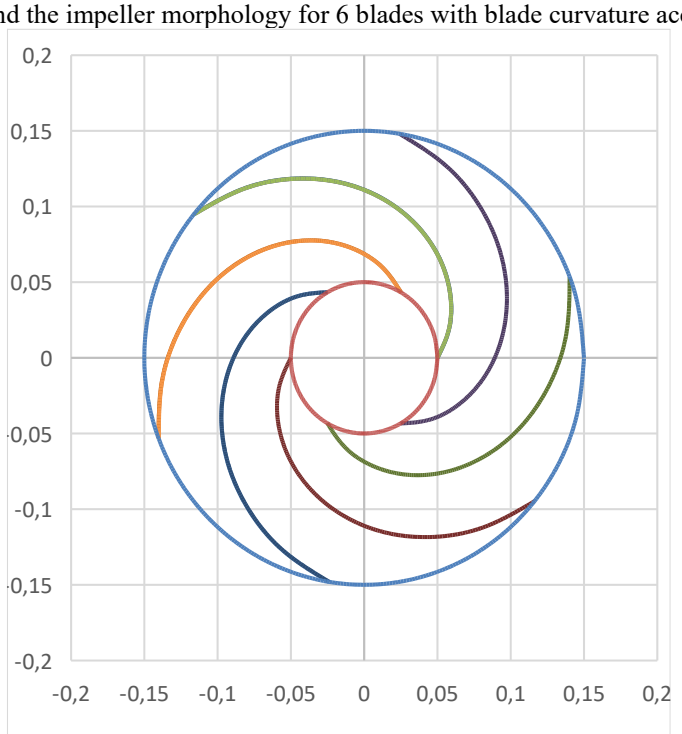

Fig.2.9. Blade profile, Impeller morphology for 6 blades with blade curvature according to Sigloch methodology.

(This work is licensed under a Creative Commons Attribution 4.0 International License.)

International Journal of Engineering Research & Technology (IJERT)
ISSN: 2278-0181
Volume 13, Issue 01 January 2024

We can obtain an alternative blade thickness by choosing an exponential form for the blades' curvature. The results are shown in Table VIII and Fig.2.10.

TABLE VIII. BLADE THICKNESS CONFIGURATION FOR EXPONENTIAL FORM FOR THE CURVATURE OF THE BLADES.

y_a	φ_{o1}	φ_1	r_1
0	0°	0°	0,074409
0,033329	Wrap angle	23,51429°	0,083576
0,064696	141,9887°	44,25575°	0,092743
0,090556		62,72826°	0,10191
0,109134		79,30663°	0,111077
0,119917		94,27784°	0,120244
0,123208		107,8671°	0,129411
0,119777		120,2548°	0,138579
0,110618		131,5881°	0,147746
0,096785		141,9887°	0,156913

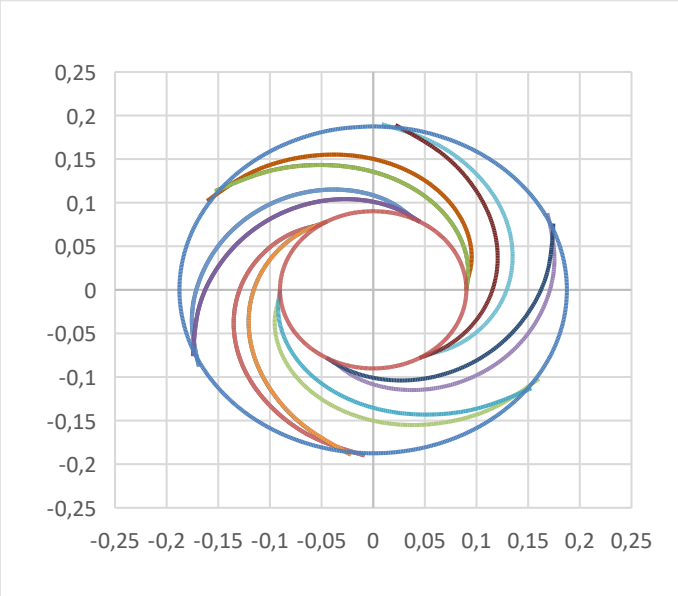

Fig.2.10. Two-dimensional diagram of the impeller [12] , blade thickness morphology by creating another blade of different curvature to the original one -for6 blades- according to the Sigloch or Menny methodology for the same wrap angle.

With different wrap angle and blade thickness on the outlet side we would have different blade curvature distributions as shown in Tables IX-XI and Figs.2.11-2.12.

TABLE IX. Blade curvature distribution with different wrap angle and blade thickness on the outlet.

x_a	y_a	φ_{o1}	φ_1	r_1
0,0744	0	0°	0°	0,0744
0,0758	0,0353	Wrap angle	24,9699°	0,0836
0,0622	0,0688	157,33°	47,9134°	0,0927
0,0368	0,095		68,8893°	0,1019
0,004	0,111		87,9635°	0,1111
-0,031	0,1161		105,206°	0,1202
-0,066	0,1114		120,689°	0,1294
-0,097	0,099		134,487°	0,1386
-0,123	0,0813		146,674°	0,1477
-0,145	0,0607		157,326°	0,1569

(This work is licensed under a Creative Commons Attribution 4.0 International License.)

International Journal of Engineering Research & Technology (IJERT)
ISSN: 2278-0181
Volume 13, Issue 01 January 2024

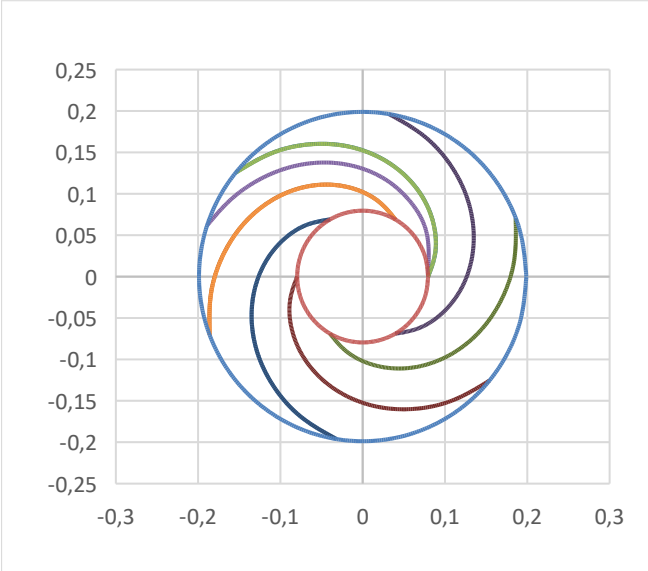

Fig.2.11. Morphologies of blade thickness at the exit with the creation of another blade with a different curvature from the original, according to the Menny methodology for another wrap angle

TABLE X. MENNY METHOD FOR BLADE SHAPE CONFIGURATION

r_x	Δr_x	b_x	w_x	cx_m	$\Delta\varphi$	φ
0,074409	0	0,04433	15,92	4,02	0	0°
0,083438	0,009167	0,042088	15,45	3,78	24,96	24,9°
0,092466	0,009167	0,039846	14,97	3,6	22,94	47,9°
0,101495	0,009167	0,037605	14,5	3,48	20,97	68,8°
0,110524	0,009167	0,035363	14,03	3,4	19,07	87,9°
0,119553	0,009167	0,033121	13,56	3,35	17,24	105,2°
0,128581	0,009167	0,03088	13,09	3,34	15,48	120,6°
0,13761	0,009167	0,028638	12,62	3,36	13,79	134,4°
0,146639	0,009167	0,026396	12,15	3,42	12,19	146,6°
0,155667	0,009167	0,024155	11,68	3,52	10,65	157,3°

The camber line profiles of impellers with different blade wrap angle φ_w according to [10], are described in Table XI and Fig.2.12.

TABLE XI. BLADE SHAPE CONFIGURATION USING DIFFERENT ALGORITHMIC FUNCTIONS AND WITH DIFFERENT WRAP ANGLES IN DETERMINING THEIR CURVATURE Φ AS A FUNCTION OF THE BLADE ANGLES B.

r"	β linear	φ	x_a	y_a
0,07954	17,29478	0	0,079539939	0
0,092797	17,64068	27,80325	0,082094294	0,043264
0,106053	17,98657	50,823124	0,067032551	0,082182
0,11931	18,33247	70,185765	0,040512377	0,112221
0,132567	18,67837	86,667782	0,007806968	0,132336
0,145823	19,02426	100,82799	-0,02726674	0,143251
0,15908	19,37016	113,08217	-0,06222094	0,146407
0,172337	19,71605	123,74807	-0,09558327	0,143401
0,185593	20,06195	133,07401	-0,12658977	0,13572
0,19885	20,40784	141,25763	-0,15494082	0,12

(This work is licensed under a Creative Commons Attribution 4.0 International License.)

International Journal of Engineering Research & Technology (IJERT)
ISSN: 2278-0181
Volume 13, Issue 01 January 2024

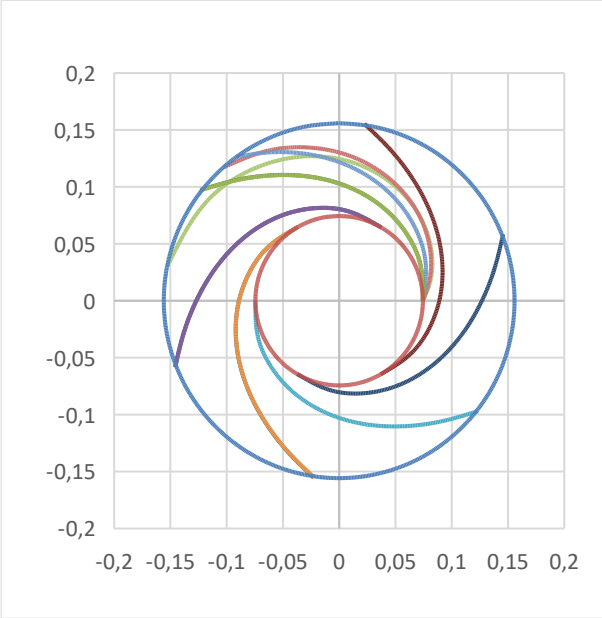

Fig.2.12. Various blades of different algorithmic functions and with different wrap angles in determining their curvature φ as a function of the blade angles β.

F. Geometry and Coordinates of Spiral Shell and Diffuser

For the design of the Spiral Shell and the Diffuser, the procedure described in [6] and [11] is followed. The geometrical results obtained are shown in Tables XII-XIV and Figs. 2.13-2.14.

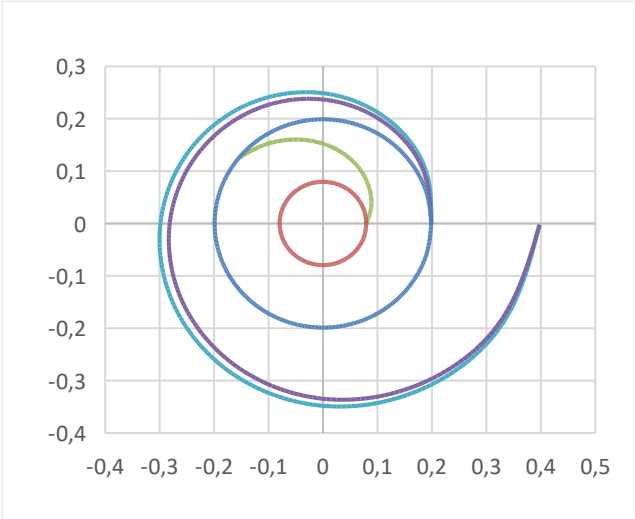

Fig.2.13. The spiral shell geometry

(This work is licensed under a Creative Commons Attribution 4.0 International License.)

International Journal of Engineering Research & Technology (IJERT)
ISSN: 2278-0181
Volume 13, Issue 01 January 2024

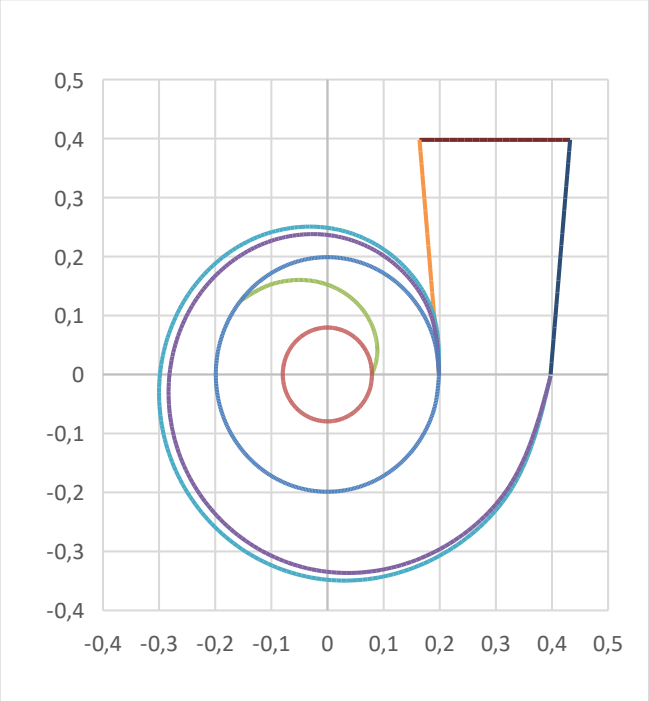

Fig.2.14. The diffuser geometry

TABLE XII. Geometry and coordinates' models for the Spiral Shell

The Logarithmic-Shaped Spiral Model	The Archimedes" Shaped Spiral Model
Shell in the form	Shell in the form
$r=a\cdot\exp(c\cdot\theta)$	$r=a\cdot r_2 + c\cdot\theta$
with the boundary conditions	with the boundary conditions
$r=r_2$ for $\theta=360$	$r=r_2$ for $\theta=360$
$r=2\cdot r_2$ for $\theta=720$	$r=2\cdot r_2$ for $\theta=720$

TABLE XIII. Spiral shell geometry

θ	r	x_r	y_r	θ	r	x_r	y_r
360	0,19	0,19	-0,0006	360	0,19	0,19	-0,00063
390	0,21	0,18	0,1	390	0,22	0,19	0,107066
420	0,22	0,11	0,19	420	0,23	0,11	0,200478
450	0,24	0,0009	0,24	450	0,24	0,0009	0,24856
480	0,25	0,12	0,21	480	0,26	-0,13	0,230173
510	0,26	-0,22	0,13	510	0,28	-0,24	0,141951
540	0,28	-0,28	0,0013	540	0,29	-0,29	0,001425
570	0,29	-0,26	-0,14	570	0,31	-0,27	-0,15605
600	0,31	-0,15	-0,27	600	0,33	-0,16	-0,28613
630	0,33	-0,0018	-0,33	630	0,34	-0,0019	-0,34798
660	0,35	0,17	-0,30	660	0,36	0,18	-0,31678
690	0,37	0,323	-0,18	690	0,38	0,32	-0,19258
720	0,39	0,39	-0,002	720	0,39	0,39	-0,00253

(This work is licensed under a Creative Commons Attribution 4.0 International License.)

International Journal of Engineering Research & Technology (IJERT)
ISSN: 2278-0181
Volume 13, Issue 01 January 2024

TABLE XIV. Geometry and coordinates of the diffuser (Diffuser angle θ=4)

A		B		C		D
x	y	x	y	x	y	x
r_2	0	$2\cdot r_2$	0	$r_2-2\cdot r_2\cdot\tan\theta$	$2\cdot r_2$	$2\cdot r_2+2r_2\cdot\tan\theta$
0,19885	0	0,3977	0	0,1710541	0,3977	0,425495

	Diffuser walls				Discharge Nozzles	
	AC		BD		CD	
	x	y	x	y	x	y
	0,19885	0	0,3977	0	0,171054	0,4
	0,171054	0,3977	0,425495	0,3976997	0,425495	0,4

II. MODELLING PUMP PERFORMANCE

Since in the previous section we obtained to design a pump using our model, it would be nice if we could have an estimate of the usual performance characteristics of this pump, ie efficiency, head and cavitation height in relation to the pump's discharge.
The best way to have an estimate of these critical parameters of the pump we designed is obviously to construct this pump and test it in the test rig. However, this is a quite costly and time-consuming procedure. An alternative way is to use or develop empirical relationships for the performance of our pump based on the performance measurements of a number of commercial pumps from various manufacturers that have published performance measurements. At the end you should compare our model predictions with these measurements. We do this in subchapter A for head and efficiency and in subchapter B for cavitation height.

A. Head and efficiency prediction

Based on the logic we described just before we selected 9 pumps whose design features are shown in Table XV. The published performance maps of these pumps digitized using appropriate software. Using the digitized performance maps we proceeded to develop some useful relationships for the efficiency curve (subsection 1) and head (subsection 2). In subsection 3, the predictions of the new relationships we propose are compared with the measurement data of the 9 pumps.

(This work is licensed under a Creative Commons Attribution 4.0 International License.)

International Journal of Engineering Research & Technology (IJERT)
ISSN: 2278-0181
Volume 13, Issue 01 January 2024

TABLE XV. DESIGN PARAMETERS FOR THE SELECTED PUMPS.

Pump parameters	Ref.[19] Pump	Ref.[20] Pump	Ref.[21] Pump	Ref.[22] Pump	Ref.[23] Pump	Ref.[24] Pump	Ref.[25] Pump	Ref.[26] Pump	Ref.[27] Pump
Q_{BEP} (m^3/h)	40	10,54	200	2,88	4,8	550	50	144	4500
Q_{BEP} (m^3/s)	0,01111	0,0029	0,0555	0,0008	0,0013	0,1527	0,01388	0,04	1,25
Q_{max}	80	21,09	400	5,78	9,6	1100	100	288	9000
H_{BEP}	30	16	32	4,8	11	50	35	60	60
$H_{shut\ off}$	35,1	18,7	37,44	5,616	12,87	58,5	40,95	70,2	70,2
n	2850	2900	1480	1500	2800	1480	2850	1800	600
n_q	23,4	19,62	25,92	13,08	16,92	30,76	23,34	16,69	31,11
n_{spec}	0,39	0,327	0,432	0,218	46,666	24,66	47,5	30	10
D	0,17	0,1	0,3146	0,06	0,0707	0,47	0,18	0,2759	1,0933
D_2	168	95	322	120	105	420	174	320	1100
D_1	70	45	148	40	20	200	74	145	450
z	6	6	6	6	8	6	6	7	6
b_2	12	8	12	15	5,2	34	12	12	100
β_2	11	40	25	20	11	26	31	28	37
β_1	9,32	33,89	21,18	10	9,32	22,03	37	11,6	21

Where:
Q_{BEP} : Design flow rate
Q_{max} : Maximum discharge (m^3/h)
D: Impeller diameter (m)
n_{spec} : Specific speed (r/min)
n: Rotational speed (r/min)
D_1: Impeller inlet diameter (mm)
D_2: Impeller outlet diameter (mm)
b_2: Blade's width in the impeller outlet (mm)
H_{BEP}: Head at BEP (best efficiency point) in meters

TABLE XVI. SOME CALCULATED PARAMETERS FOR THE SELECTED PUMPS.

Pump parameters	Ref.[19] Pump	Ref.[20] Pump	Ref.[21] Pump	Ref.[22] Pump	Ref.[23] Pump	Ref.[24] Pump	Ref.[25] Pump	Ref.[26] Pump	Ref.[27] Pump
c_{1m}	2,83	1,93	3,05	1,009	1,52	4,11	4,11	3,54	4,53
c_{2m}	2	1,153	1,995	0,753	1,230	2,602	2,076	2,411	2,763
σ	0,986	0,993	0,991	0,983	0,989	0,991	0,994	0,984	0,989
c_{2u}	14,40	12,94	20,44	7,19	8,88	26,83	22,21	25,15	30,50
u_2	25,05	14,41	24,93	9,42	15,38	32,53	25,95	30,14	34,54
u_1	10,44	6,82	11,46	3,14	2,93	15,49	11,03	13,65	14,13

(This work is licensed under a Creative Commons Attribution 4.0 International License.)

International Journal of Engineering Research & Technology (IJERT)
ISSN: 2278-0181
Volume 13, Issue 01 January 2024

Where:

c_{2m}: inlet flow velocity (m/s), n_q<24 r/min
c_{2u}: swirl velocity at the outlet (m/s)
σ: the slip value

1) Proposed relations for predicting head curves

The calculational procedure for predicting the manometric head curves for the 9 selected pumps of Table XV, has as follows:

$$H_{shut\ off} = 1{,}17 \cdot H_{BEP} \quad (3.1)$$

Where the head at BEP (best efficiency point) H_{BEP} is known from the experiment. However H_{BEP} can also be calculated by the following empirical formula:

$$H_{BEP} = 0.575\, u_2^2 / g \quad (3.2)$$

By knowing H_{BEP} in the present work we propose the following formulas for predicting the variation of head vs the flow rate:

$$H = H_{shutoff} \cdot [\cos(0{,}5 \cdot 1{,}57 \cdot j)]^{0{,}5} \quad (3.3a)$$

$$H = H_{shutoff} \cdot [1 - 0.2 \cdot j^2] \quad (3.3b)$$

$$H = H_{shutoff} \cdot [1 - 0.125\, j^3] \quad (3.3c)$$

$$H = H_{shutoff} \cdot [2 - \exp(0.15\, j^2)] \quad (3.3d)$$

$$H = H_{shutoff} \cdot erfc(0.17 \cdot j^2) \quad (3.3e)$$

$$H = H_{shutoff} \cdot [Besselj0(j)]^{0{,}72} \quad (3.3f)$$

$$H = H_{shutoff} \cdot \cos(0{,}5 \cdot j) \quad (3.3g)$$

Where erfc is the complementary error function given by:

erfc(z)=1-erf(z)

and j is given by:

$$j = Q/Q_{BEP} \quad (3.4)$$

The discharge at BEP (best efficiency point) Q_{BEP} is known from the experiment. However Q_{BEP} can also be calculated by the following empirical formula:

$$Q_{BEP} = 3600 \cdot (0.1 \cdot \pi \cdot u_2 \cdot b_2 \cdot D_2^{3.695})^{0.49} \quad (3.5)$$

where:

Q_{BEP} in m^3/h

u_2 in m/sec and

D_2 and b_2 in m

(This work is licensed under a Creative Commons Attribution 4.0 International License.)

International Journal of Engineering Research & Technology (IJERT)
ISSN: 2278-0181
Volume 13, Issue 01 January 2024

a) Calculational results for head predictions.

For predicting the head-discharge variation of the selected pumps of Table XV we use the formulas (3.3a) to (3.3g). The calculational results are shown in Tables XVIII to XXVI and Figs. 3.1 to 3.17.

TABLE XVII. PRESENT MODEL PREDICTIONS FOR [19] PUMP CHARACTERISTICS

Ref.[19] Pump			Predictions						
Q (m^3/h)	j= Q/Q_{BEP}	H (m)	Eq.(3.3a)	Eq.(3.3b)	Eq.(3.3c)	Eq.(3.3d)	Eq.(3.3e)	Eq.(3.3f)	Eq.(3.3g)
0	0	35,2	35,1	35,1	35,1	35,1	35,1	35,1	35,1
10	0,26	35	34,74	34,64	35,03	34,75	34,66	34,69	34,81
20	0,5	34	33,67	33,25	34,51	33,69	33,33	33,45	33,95
30	0,75	32	31,85	30,95	33,1	31,84	31,13	31,42	32,54
40	1	29	29,22	27,72	30,37	29,1	28,09	28,64	30,58
50	1,25	25	25,67	23,56	25,85	25,29	24,31	25,15	28,13

TABLE XVIII. PRESENT MODEL PREDICTIONS FOR [20] PUMP CHARACTERISTICS

Ref.[20] Pump			Predictions						
Q (m^3/h)	j= Q/Q_{BEP}	H (m)	Eq.(3.3a)	Eq.(3.3b)	Eq.(3.3c)	Eq.(3.3d)	Eq.(3.3e)	Eq.(3.3f)	Eq.(3.3g)
0	0	17,5	17,25	17,26	17,26	17,26	17,26	17,26	17,26
7,2	0,83	15,5	15,35	14,84	15,99	15,34	14,95	15,12	15,77
14,4	1,67	8,3	8,69	7,58	7,13	8,24	8,63	9,13	11,55

TABLE XIX. Present model predictions for [21] pump characteristics

Ref.[21] Pump			Predictions						
Q (m^3/h)	j= Q/Q_{BEP}	H (m)	Eq.(3.3a)	Eq.(3.3b)	Eq.(3.3c)	Eq.(3.3d)	Eq.(3.3e)	Eq.(3.3f)	Eq.(3.3g)
0	0	36,3	37,44	37,44	37,44	37,44	37,44	37,44	37,44
50	0,25	36	37,07	36,97	37,37	37,09	36,99	37,02	37,15
100	0,5	35	35,98	35,57	36,86	36,01	35,65	35,77	36,28
150	0,75	33,5	34,14	33,23	35,47	34,14	33,41	33,71	34,84
200	1	31	31,48	29,95	32,76	31,38	30,33	30,88	32,86
250	1,25	26,5	27,91	25,74	28,3	27,55	26,48	27,33	30,36
275	1,37	24	25,71	23,28	25,27	25,16	24,32	25,3	28,93

(This work is licensed under a Creative Commons Attribution 4.0 International License.)

International Journal of Engineering Research & Technology (IJERT)
ISSN: 2278-0181
Volume 13, Issue 01 January 2024

TABLE XX. PRESENT MODEL PREDICTIONS FOR [22] PUMP CHARACTERISTICS

Ref.[22] Pump			Predictions						
Q (m^3/h)	j= Q/Q_{BEP}	H (m)	Eq.(3.3a)	Eq.(3.3b)	Eq.(3.3c)	Eq.(3.3d)	Eq.(3.3e)	Eq.(3.3f)	Eq.(3.3g)
0	0	6	5,61	5,62	5,62	5,62	5,62	5,62	5,62
0,72	0,25	5,9	5,56	5,55	5,61	5,56	5,55	5,55	5,57
1,44	0,5	5,7	5,39	5,34	5,53	5,4	5,35	5,36	5,44
2,16	0,75	5,4	5,12	4,98	5,32	5,12	5,01	5,06	5,23
2,88	1	4,9	4,72	4,49	4,91	4,71	4,55	4,63	4,93
3,6	1,25	4,3	4,18	3,86	4,24	4,13	3,97	4,1	4,55
4,32	1,5	3,5	3,47	3,09	3,25	3,36	3,31	3,47	4,11

TABLE XXI. PRESENT MODEL PREDICTIONS FOR [23] PUMP CHARACTERISTICS

Ref.[23] Pump			Predictions						
Q (m^3/h)	j= Q/Q_{BEP}	H (m)	Eq.(3.3a)	Eq.(3.3b)	Eq.(3.3c)	Eq.(3.3d)	Eq.(3.3e)	Eq.(3.3f)	Eq.(3.3g)
0	0	12,4	12,87	12,87	12,87	12,87	12,87	12,87	12,87
2	0,42	12,1	12,52	12,42	12,75	12,53	12,44	12,47	12,59
4	0,83	11,2	11,46	11,08	11,94	11,46	11,16	11,29	11,77
6	1,25	9,2	9,59	8,85	9,73	9,47	9,1	9,4	10,44
8	1,66	6	6,55	5,72	5,42	6,22	6,49	6,86	8,65

TABLE XXII. PRESENT MODEL PREDICTIONS FOR [24] PUMP CHARACTERISTICS

Ref.[24] Pump			Predictions						
Q (m^3/h)	j= Q/Q_{BEP}	H (m)	Eq.(3.3a)	Eq.(3.3b)	Eq.(3.3c)	Eq.(3.3d)	Eq.(3.3e)	Eq.(3.3f)	Eq.(3.3g)
0	0	61,3	58,5	58,5	58,5	58,5	58,5	58,5	58,5
200	0,36	60	57,3	56,95	58,15	57,32	57,01	57,11	57,53
300	0,55	58	55,79	55,01	57,31	55,82	55,15	55,38	56,33
400	0,73	56	53,64	52,29	55,67	53,65	52,56	52,99	54,66
500	0,91	53	50,84	48,8	52,98	50,75	49,25	49,96	52,54
600	1,09	49	47,31	44,53	48,95	47,02	45,28	46,31	49,98
700	1,28	44	42,97	39,48	43,34	42,34	40,71	42,09	47,01
800	1,46	38	37,64	33,66	35,87	36,56	35,67	37,32	43,65

(This work is licensed under a Creative Commons Attribution 4.0 International License.)

International Journal of Engineering Research & Technology (IJERT)
ISSN: 2278-0181
Volume 13, Issue 01 January 2024

TABLE XXIII. PRESENT MODEL PREDICTIONS FOR [25] PUMP CHARACTERISTICS

Ref.[25] Pump			Predictions						
Q (m^3/h)	j= Q/Q_{BEP}	H (m)	Eq.(3.3a)	Eq.(3.3b)	Eq.(3.3c)	Eq.(3.3d)	Eq.(3.3e)	Eq.(3.3f)	Eq.(3.3g)
0	0	40	40,95	40,95	40,95	40,95	40,95	40,95	40,95
10	0,2	39,5	40,7	40,62	40,91	40,7	40,64	40,66	40,75
20	0,4	39,2	39,94	39,64	40,62	39,96	39,69	39,78	40,13
30	0,6	38,5	38,66	38	39,84	38,68	38,13	38,32	39,12
40	0,8	37,5	36,84	35,71	38,33	36,82	35,94	36,31	37,72
50	1	35,5	34,44	32,76	35,83	34,32	33,17	33,77	35,94
60	1,2	32	31,41	29,16	32,1	31,08	29,86	30,73	33,8
70	1,4	28	27,61	24,9	26,9	26,95	26,11	27,21	31,32

TABLE XXIV. PRESENT MODEL PREDICTIONS FOR [26] PUMP CHARACTERISTICS

Ref.[26] Pump			Predictions						
Q (m^3/h)	j= Q/Q_{BEP}	H (m)	Eq.(3.3a)	Eq.(3.3b)	Eq.(3.3c)	Eq.(3.3d)	Eq.(3.3e)	Eq.(3.3f)	Eq.(3.3g)
0	0	65	62,01	62,01	62,01	62,01	62,01	62,01	62,01
72	0,5	63	59,61	58,91	61,04	59,64	59,04	59,24	60,08
144	1	54	52,15	49,61	54,26	51,97	50,23	51,14	54,42
216	1,5	39	38,39	34,11	35,85	37,12	36,5	38,29	45,37
252	1,75	27	27,44	24,03	20,47	25,85	28,62	30,25	39,75

TABLE XXV. PRESENT MODEL PREDICTIONS FOR [27] PUMP CHARACTERISTICS

Ref.[27] Pump			Predictions						
Q (m^3/h)	j= Q/Q_{BEP}	H (m)	Eq.(3.3a)	Eq.(3.3b)	Eq.(3.3c)	Eq.(3.3d)	Eq.(3.3e)	Eq.(3.3f)	Eq.(3.3g)
0	0	68	70,2	70,2	70,2	70,2	70,2	70,2	70,2
2000	0,46	67	67,88	67,21	69,34	67,92	67,33	67,52	68,34
3000	0,69	66	64,95	63,47	67,29	64,97	63,76	64,22	66,04
4000	0,92	63	60,75	58,24	63,3	60,63	58,81	59,68	62,86
5000	1,15	57	55,15	51,51	56,73	54,69	52,58	53,96	58,84
6000	1,38	50	47,89	43,29	46,92	46,82	45,28	47,15	54,04
7000	1,62	40	38,34	33,57	33,23	36,58	37,24	39,3	48,53

(This work is licensed under a Creative Commons Attribution 4.0 International License.)

International Journal of Engineering Research & Technology (IJERT)
ISSN: 2278-0181
Volume 13, Issue 01 January 2024

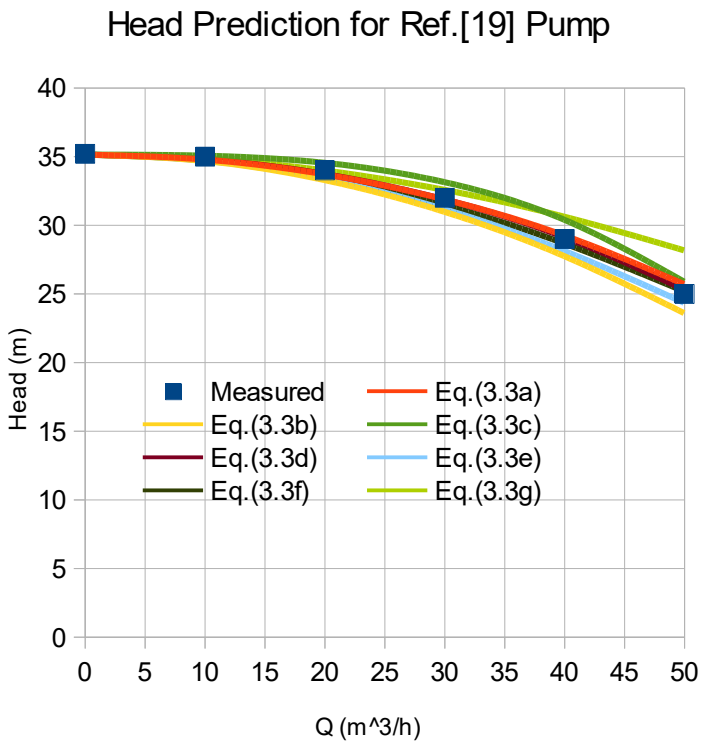

Fig.3.1. Using present model to predict [19] pump head

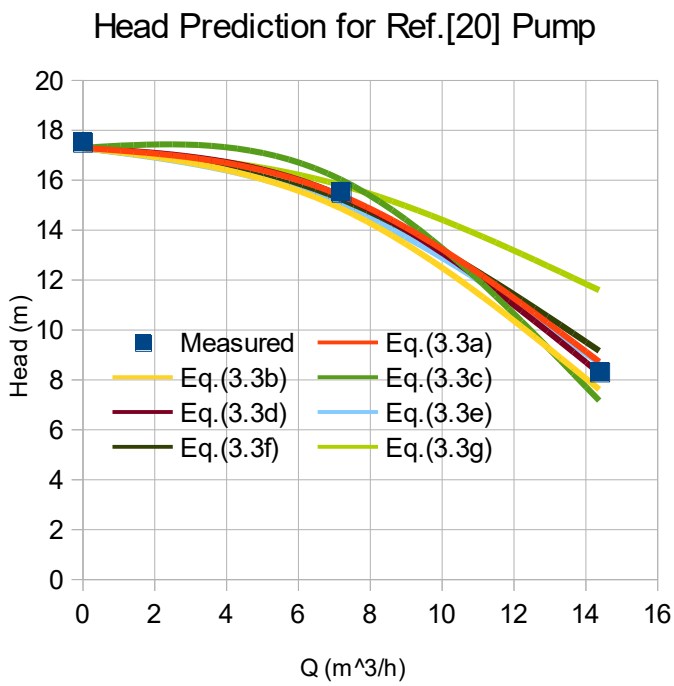

Fig.3.2. Using present model to predict [20] pump head

(This work is licensed under a Creative Commons Attribution 4.0 International License.)

International Journal of Engineering Research & Technology (IJERT)
ISSN: 2278-0181
Volume 13, Issue 01 January 2024

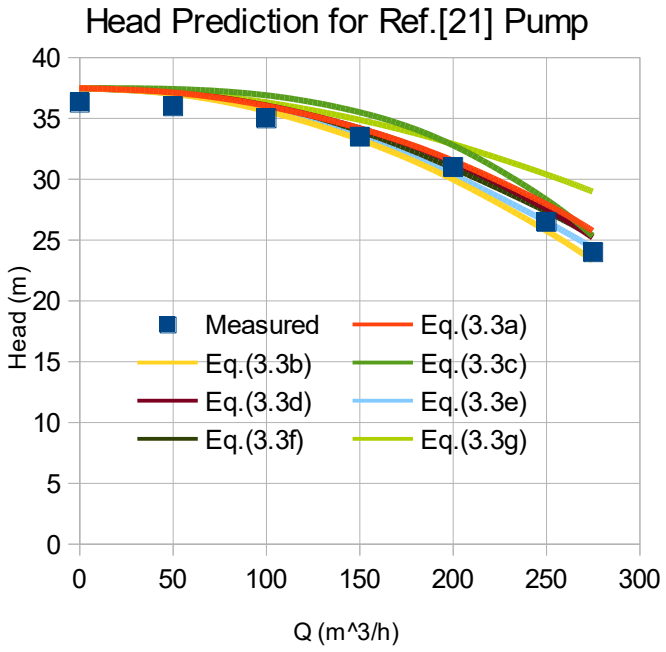

Fig.3.3. Using present model to predict [21] pump head

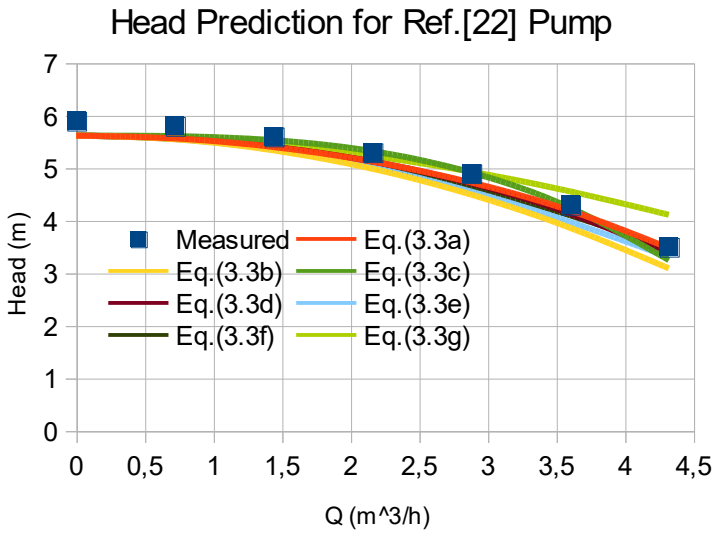

Fig.3.4. Using present model to predict [22] pump head

(This work is licensed under a Creative Commons Attribution 4.0 International License.)

International Journal of Engineering Research & Technology (IJERT)
ISSN: 2278-0181
Volume 13, Issue 01 January 2024

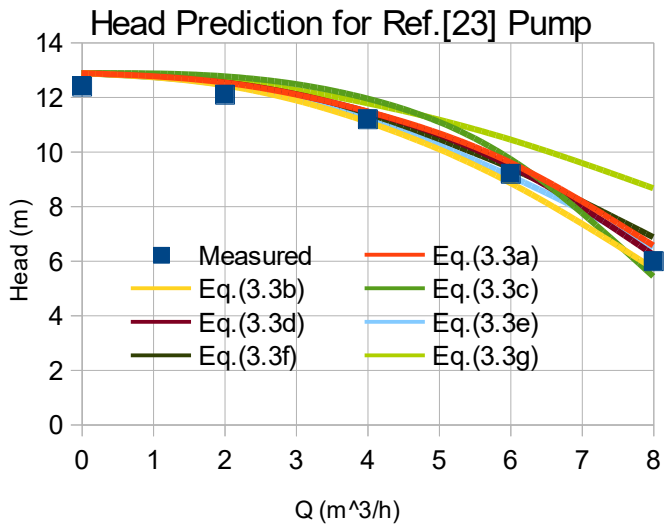

Fig.3.5. Using present model to predict [23] pump head

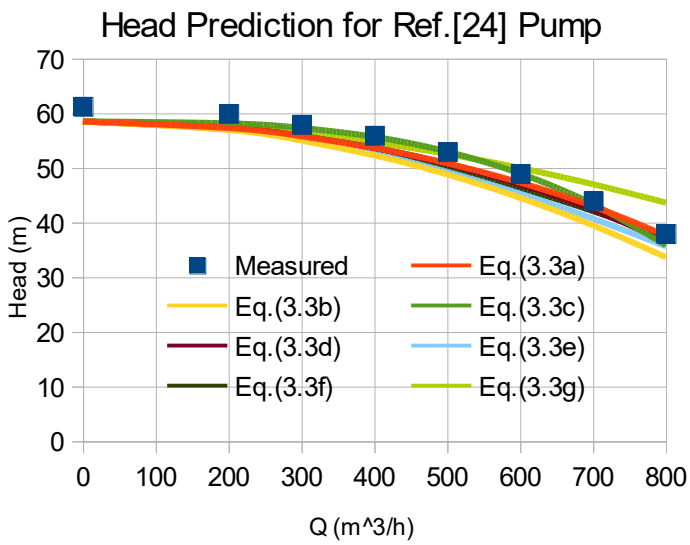

Fig.3.6. Using present model to predict [24] pump head.

(This work is licensed under a Creative Commons Attribution 4.0 International License.)

International Journal of Engineering Research & Technology (IJERT)
ISSN: 2278-0181
Volume 13, Issue 01 January 2024

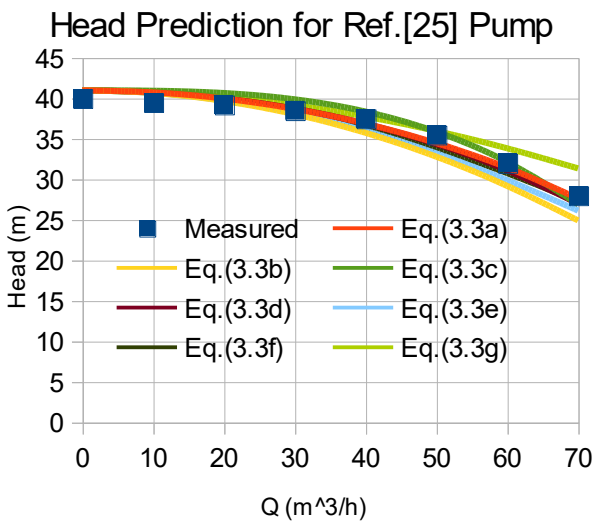

Fig.3.7. Using present model to predict [25] pump head

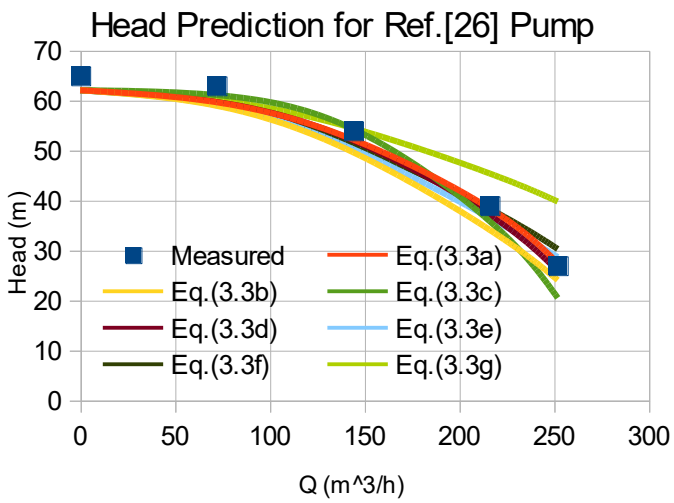

Fig.3.8. Using present model to predict [26] pump head

(This work is licensed under a Creative Commons Attribution 4.0 International License.)

International Journal of Engineering Research & Technology (IJERT)
ISSN: 2278-0181
Volume 13, Issue 01 January 2024

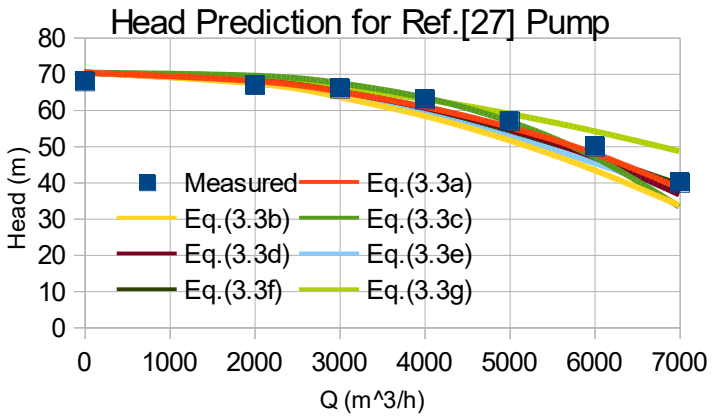

Fig.3.9. Using present model to predict [27] pump head

2) Proposed relations for predicting efficiency curves

The calculational procedure for predicting the pump efficiency curves for the 9 selected pumps of Table XV, has as follows:

The mechanical efficiency is:

$$\eta_m = \frac{1}{1.1 + \frac{1}{n_q}} \tag{3.6}$$

The volumetric efficiency for $n_q < 23{,}5$ r/min is:

$$\eta_q = \frac{1}{1 + \frac{2}{n_q^{0.66}}} \tag{3.7}$$

while the volumetric efficiency for $n_q > 23{,}5$ r/min is:

$$\eta_q = \frac{1}{1 + \frac{0.2}{n_q^{0.66}}} \tag{3.8}$$

The hydraulic efficiency is:

$$\eta_h = \frac{1}{1.1 + \frac{0.9}{n_q^{0.66}}} \tag{3.9}$$

As a result the overall efficiency is:

$$\eta_{max} = \eta_m \cdot \eta_q \cdot \eta_h \tag{3.10}$$

(This work is licensed under a Creative Commons Attribution 4.0 International License.)

International Journal of Engineering Research & Technology (IJERT)
ISSN: 2278-0181
Volume 13, Issue 01 January 2024

Summary of calculations is shown in Table XVII.

TABLE XXVI. EFFICIENCY CALCULATIONS

Pump parameters	Ref.[19] Pump	Ref.[20] Pump	Ref.[21] Pump	Ref.[22] Pump	Ref.[23] Pump	Ref.[24] Pump	Ref.[25] Pump	Ref.[26] Pump	Ref.[27] Pump
η_q	0,8	0,78	0,977	0,731	0,731	0,979	0,975	0,762	0,979
η_h	0,96	0,943	0,975	0,932	0,873	0,938	0,901	0,920	0,974
η_m	0,88	0,868	0,878	0,850	0,862	0,882	0,875	0,862	0,883
η_{max}	0,67	0,639	0,837	0,579	0,551	0,811	0,769	0,604	0,843

In the present work we propose the following formulas for predicting the variation of pump efficiency vs the flow rate:

$$\eta = \eta_{max} \cdot \sin(1{,}57 \cdot j) \quad (3.11a)$$

$$\eta = 3.18 \cdot \eta_{max} \cdot [-0.49 \cdot j + 1.02 \cdot erf(0.89 \cdot j)] \quad (3.11b)$$

$$\eta = \eta_{max} \cdot j \cdot (2 - j) \quad (3.11c)$$

$$\eta = \eta_{max} \cdot [erf(1.5 \cdot j)] \cdot [1.14 - erf(0.12 \cdot j^3)] \quad (3.11d)$$

$$\eta = \eta_{max} \cdot [erf(6.28 \cdot j)] \cdot [\sin(1.57 \cdot j)]^{0.8} \quad (3.11e)$$

$$\eta = \eta_{max} \cdot [\sin(1{,}57 \cdot j)]^{0.8} \quad (3.11f)$$

$$\eta = \eta_{max} \cdot [1 - (1 - j)^2] \quad (3.11g)$$

Where *erf* is the error function and the factor *j* is given by:

a) Calculational results for efficiency predictions.

For predicting the efficiency-discharge variation of the selected pumps of Table XV we use the formulas (3.11a) to (3.11g). The calculational results are shown in Tables XVIII to XXVI and Figs. 3.1 to 3.17. The symbols in the first three columns in Tables XVIII to XXVI are:

Q: Flow rate (m^3/h)
$j = Q/Q_{BEP}$
H: Head (m)

TABLE XXVII. PRESENT MODEL PREDICTIONS FOR [19] PUMP CHARACTERISTICS

Ref.[19] Pump			Predictions						
Q	j	H	Eq. 3.11a	Eq. 3.11b	Eq. 3.11c	Eq. 3.11d	Eq. 3.11e	Eq. 3.11f	Eq. 3.11g
0	0	0	0	0	0	0	0	0	0
10	0,26	0,29	0,26	0,28	0,3	0,3	0,31	0,32	0,3
20	0,51	0,5	0,48	0,51	0,51	0,53	0,52	0,52	0,51
30	0,77	0,63	0,63	0,65	0,63	0,63	0,63	0,63	0,63
40	1,03	0,65	0,67	0,67	0,67	0,64	0,67	0,67	0,67
50	1,28	0,6	0,61	0,6	0,62	0,58	0,62	0,62	0,62

(This work is licensed under a Creative Commons Attribution 4.0 International License.)

International Journal of Engineering Research & Technology (IJERT)
ISSN: 2278-0181
Volume 13, Issue 01 January 2024

TABLE XXVIII. Present model predictions for [21] pump characteristics

Ref.[21] Pump			Predictions						
Q	j	H	Eq. 3.11a	Eq. 3.11b	Eq. 3.11c	Eq. 3.11d	Eq. 3.11e	Eq. 3.11f	Eq. 3.11g
0	0	0	0	0	0	0	0	0	0
50	0,25	0,35	0,32	0,34	0,37	0,37	0,38	0,39	0,37
100	0,5	0,6	0,59	0,63	0,63	0,65	0,63	0,63	0,63
150	0,75	0,75	0,77	0,8	0,78	0,78	0,79	0,79	0,78
200	1	0,8	0,84	0,85	0,84	0,8	0,84	0,84	0,84
250	1,25	0,76	0,77	0,77	0,78	0,73	0,79	0,79	0,78
275	1,38	0,72	0,7	0,69	0,72	0,68	0,72	0,72	0,72

TABLE XXIX. PRESENT MODEL PREDICTIONS FOR [22] PUMP CHARACTERISTICS

Ref.[22] Pump			Predictions						
Q	j	H	Eq. 3.11a	Eq. 3.11b	Eq. 3.11c	Eq. 3.11d	Eq. 3.11e	Eq. 3.11f	Eq. 3.11g
0	0	0	0	0	0	0	0	0	0
0	0,25	0,25	0,22	0,24	0,25	0,26	0,26	0,27	0,25
0,72	0,5	0,43	0,41	0,43	0,43	0,45	0,44	0,44	0,43
1,44	0,75	0,53	0,54	0,55	0,54	0,54	0,54	0,54	0,54
2,16	1	0,56	0,58	0,59	0,58	0,55	0,58	0,58	0,58
2,88	1,25	0,52	0,54	0,53	0,54	0,51	0,54	0,54	0,54
3,6	1,5	0,4	0,41	0,41	0,43	0,42	0,44	0,44	0,43

TABLE XXX. PRESENT MODEL PREDICTIONS FOR [23] PUMP CHARACTERISTICS

Ref.[23] Pump			Predictions						
Q	j	H	Eq. 3.11a	Eq. 3.11b	Eq. 3.11c	Eq. 3.11d	Eq. 3.11e	Eq. 3.11f	Eq. 3.11g
0	0	0	0	0	0	0	0	0	0
2	0,42	0,34	0,34	0,36	0,36	0,38	0,37	0,37	0,36
4	0,83	0,53	0,53	0,55	0,54	0,53	0,54	0,54	0,54
6	1,25	0,51	0,51	0,51	0,52	0,48	0,52	0,52	0,52
8	1,67	0,28	0,28	0,29	0,31	0,34	0,32	0,32	0,31

TABLE XXXI. PRESENT MODEL PREDICTIONS FOR [24] PUMP CHARACTERISTICS

Ref.[24] Pump			Predictions						
Q	j	H	Eq. 3.11a	Eq. 3.11b	Eq. 3.11c	Eq. 3.11d	Eq. 3.11e	Eq. 3.11f	Eq. 3.11g
0	0			0	0	0	0	0	0
200	0,36			0,47	0,48	0,5	0,5	0,5	0,48
300	0,55	0,68	0,61	0,65	0,64	0,66	0,65	0,65	0,64
400	0,73	0,77	0,74	0,77	0,75	0,75	0,75	0,75	0,75
500	0,91	0,81	0,8	0,82	0,81	0,78	0,81	0,81	0,81
600	1,09	0,82	0,8	0,81	0,8	0,76	0,8	0,8	0,8
700	1,28	0,77	0,74	0,73	0,75	0,7	0,75	0,75	0,75
800	1,46	0,67	0,61	0,61	0,64	0,62	0,65	0,65	0,64

(This work is licensed under a Creative Commons Attribution 4.0 International License.)

International Journal of Engineering Research & Technology (IJERT)
ISSN: 2278-0181
Volume 13, Issue 01 January 2024

TABLE XXXII. PRESENT MODEL PREDICTIONS FOR [25] PUMP CHARACTERISTICS

Ref.[25] Pump			Predictions						
Q	j	H	Eq. 3.11a	Eq. 3.11b	Eq. 3.11c	Eq. 3.11d	Eq. 3.11e	Eq. 3.11f	Eq. 3.11g
0	0	0	0	0	0	0	0	0	0
10	0,2	0,3	0,24	0,26	0,28	0,28	0,28	0,3	0,29
20	0,4	0,5	0,45	0,48	0,49	0,51	0,5	0,5	0,52
30	0,6	0,64	0,62	0,65	0,65	0,66	0,65	0,65	0,68
40	0,8	0,73	0,73	0,75	0,74	0,73	0,74	0,74	0,78
50	1	0,77	0,77	0,78	0,77	0,73	0,77	0,77	0,81
60	1,2	0,75	0,73	0,73	0,74	0,69	0,74	0,74	0,78
70	1,4	0,67	0,62	0,62	0,65	0,61	0,65	0,65	0,68

TABLE XXXIII. PRESENT MODEL PREDICTIONS FOR [26] PUMP CHARACTERISTICS

Ref.[26] Pump			Predictions						
Q	j	H	Eq. 3.11a	Eq. 3.11b	Eq. 3.11c	Eq. 3.11d	Eq. 3.11e	Eq. 3.11f	Eq. 3.11g
0	0	0	0	0	0	0	0	0	0
72	0,5	0,46	0,44	0,46	0,46	0,48	0,47	0,47	0,46
144	1	0,6	0,62	0,62	0,62	0,59	0,62	0,62	0,62
216	1,5	0,45	0,44	0,44	0,46	0,45	0,47	0,47	0,46
252	1,75	0,3	0,24	0,26	0,27	0,34	0,29	0,29	0,27

TABLE XXXIV. PRESENT MODEL PREDICTIONS FOR [27] PUMP CHARACTERISTICS

Ref.[27] Pump			Predictions						
Q	j	H	Eq. 3.11a	Eq. 3.11b	Eq. 3.11c	Eq. 3.11d	Eq. 3.11e	Eq. 3.11f	Eq. 3.11g
0	0	0	0	0	0	0	0	0	0
2000	0,46	0,6	0,56	0,59	0,6	0,62	0,61	0,61	0,6
3000	0,69	0,78	0,75	0,78	0,76	0,77	0,76	0,76	0,76
4000	0,92	0,87	0,84	0,85	0,84	0,81	0,84	0,84	0,84
5000	1,15	0,86	0,82	0,82	0,82	0,77	0,82	0,82	0,82
6000	1,38	0,76	0,69	0,69	0,72	0,68	0,72	0,72	0,72
7000	1,62	0,59	0,48	0,5	0,52	0,55	0,54	0,54	0,52

(This work is licensed under a Creative Commons Attribution 4.0 International License.)

International Journal of Engineering Research & Technology (IJERT)
ISSN: 2278-0181
Volume 13, Issue 01 January 2024

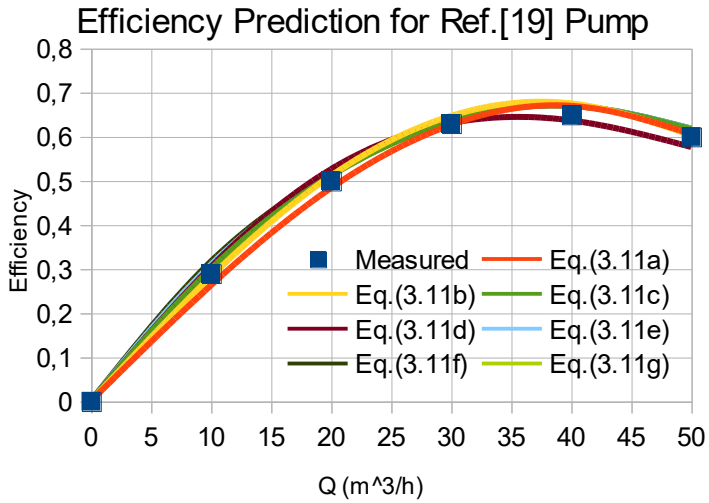

Fig.3.10. Using present model to predict [19] pump efficiency.

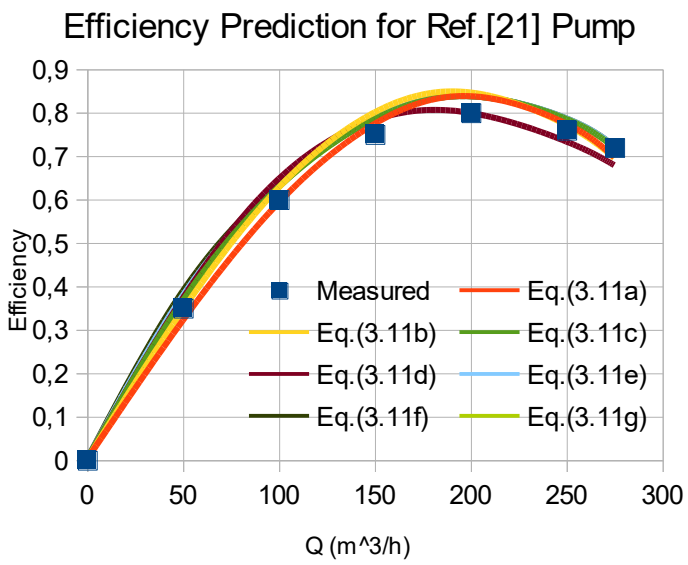

Fig.3.11. Using present model to predict [21] pump efficiency.

(This work is licensed under a Creative Commons Attribution 4.0 International License.)

International Journal of Engineering Research & Technology (IJERT)
ISSN: 2278-0181
Volume 13, Issue 01 January 2024

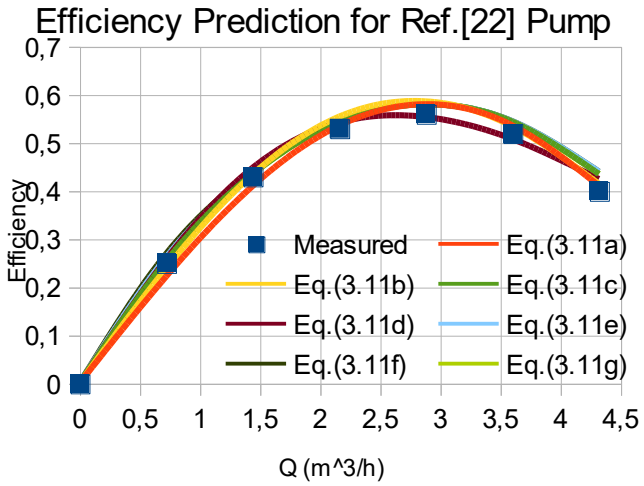

Fig.3.12. Using present model to predict [22] pump efficiency.

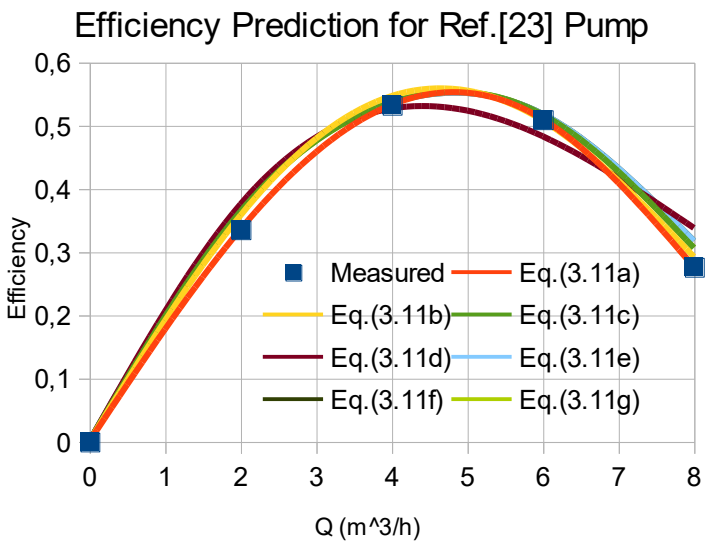

Fig.3.13. Using present model to predict [23] pump efficiency.

(This work is licensed under a Creative Commons Attribution 4.0 International License.)

International Journal of Engineering Research & Technology (IJERT)
ISSN: 2278-0181
Volume 13, Issue 01 January 2024

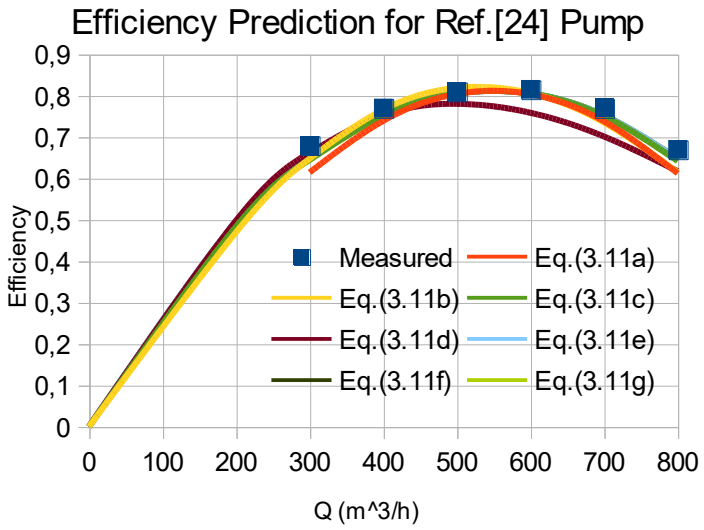

Fig.3.14. Using present model to predict [24] pump efficiency.

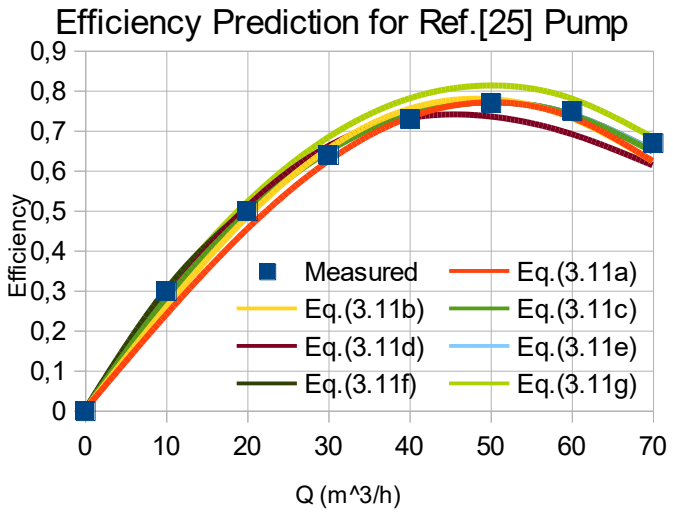

Fig.3.15. Using present model to predict [25] pump efficiency.

(This work is licensed under a Creative Commons Attribution 4.0 International License.)

International Journal of Engineering Research & Technology (IJERT)
ISSN: 2278-0181
Volume 13, Issue 01 January 2024

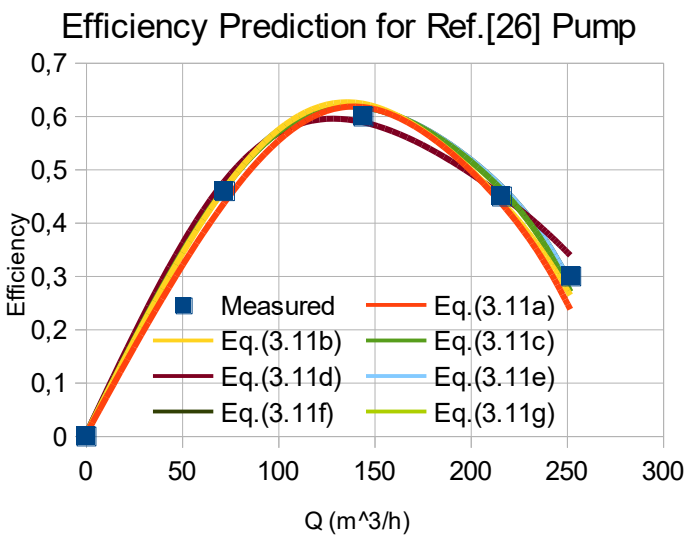

Fig.3.16. Using present model to predict [26] pump efficiency.

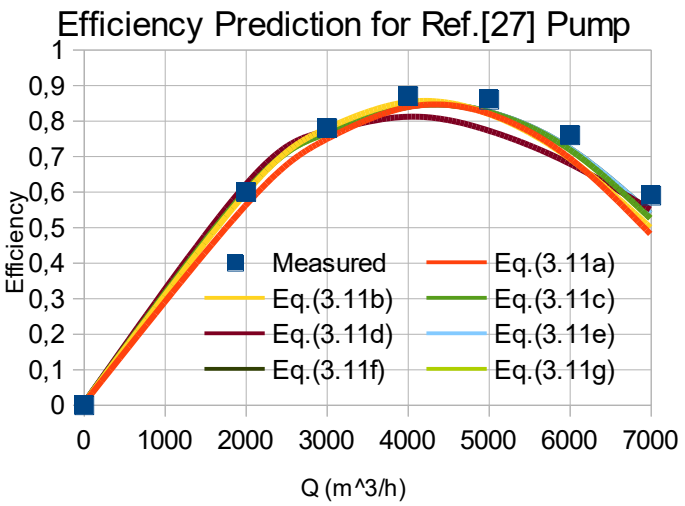

Fig.3.17. Using present model to predict [27] pump efficiency.

B. $NPSH_R$ Predictions

NPSH (Net Positive Suction Head) is a measure of the pressure experienced by a fluid on the suction side of a centrifugal pump. It is used to avoid running a pump under conditions which favour cavitation. $NPSH_R$ (NPSH Required) and $NPSH_A$ (NPSH Available) are two key NPSH values:

•$NPSH_R$ is a pump property quoted by pump manufacturers as the suction pressure at which cavitation has already reduced pump performance by 3%.

•$NPSH_A$ is a system property calculated from the suction-side system configuration. It is essentially the suction-side pressure less the vapour pressure of the pumped fluid at that point.

To avoid cavitation, it is necessary to ensure that $NPSH_A$ exceeds $NPSH_R$ by a sufficient safety margin, for example:

$NPSH_A > NPSH_R + 0.5m$.

This margin depends on the type of pump and application and may be quoted as a ratio or a head difference.

So in order to avoid cavitation problems in a pumping assembly, it is important to calculate the values of $NPSH_A$ and $NPSH_R$.

In what follows, we present methodologies for estimating both $NPSH_A$ and $NPSH_R$ as accurately as possible.

<u>$NPSH_A$ calculation [1]</u>

(This work is licensed under a Creative Commons Attribution 4.0 International License.)

International Journal of Engineering Research & Technology (IJERT)
ISSN: 2278-0181
Volume 13, Issue 01 January 2024

$NPSH_A$ can easily be calculated by the following relation:

$$NPSH_A = h_p - h_{vpa} + h_{st} - h_{fs} - h_a \quad (3.12)$$

Where:

h_p: absolute pressure head in meters on the surface of the liquid supply level

h_{vpa}: Vapor pressure of the liquid converted to meters

h_{st}: Static height in meters, difference between liquid level and established pump datum.

h_{fs}: All suction line losses converted from pressure to meters including piping entrance losses and friction losses through the pipe, valves, etc.

h_a: Acceleration head

$\sigma = NPSH/H$, Thoma's cavitation number σ

<u>$NPSH_R$ calculation</u>

Using the pump's affinity law, the cavitation problem is transformed into the following empirical formula used in the present model for estimating the variation of $NPSH_{R,x}$ in relation to the pump's flow rate:

$$NPSH_{R,x}=NPSH_{R,ref}\,(Q_x/Q_{ref})^{0.1} \quad (3.13)$$

where the reference values are known from the experiments in the test rig.

Using Eq. (3.13) we can calculate the variation of $NPSH_R$ with respect to Q for the pump we designed in II. The results are shown in Table XXVII and Figure 3.18.

TABLE XXXV. MMMM

Q/Q_{BEP}	$NPSH_{R,r}$
0	0
0,6	1,67
0,8	2,3
1	2,9
1,2	3,7

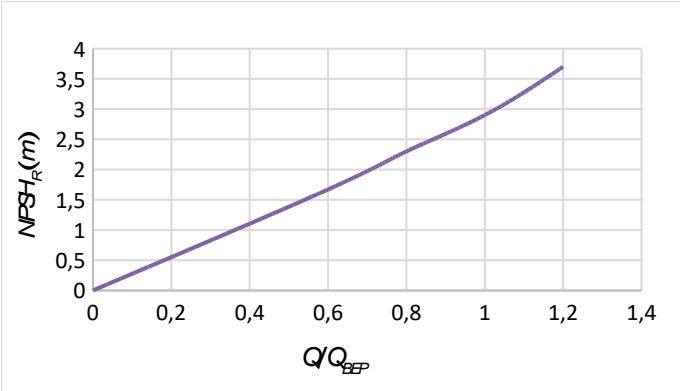

Fig. 3.18. Present model test rig centrifugal pump $NPSH_R$ variation with discharge flow.

In order to check the validity of Eq.(3.13) we selected 5 commercial pumps ([29]-[33]) for which the manufacturers provided values for the $NPSH_R$ for each pump. We then proceeded to calculate the variation of $NPSH_R$ for each pump separately. The results of the calculations are shown in Tables XXVIII to XXXII and Figures 3.19 to 3.23.

<u>Comparison of cavitation prediction performances for some centrifugal pumps</u>

TABLE XXXVI. PREDICTING $NPSH_R$ FOR REF.[29] EXPERIMENT

Q/Q_{BE}	$NPSH_{R,ref}$	Experiment	Prediction
0	0		
0,6	2,1	2	2,09
0,8	2,8	2,65	2,79
1	3,5	3,3	3,49
1,2	4,2	4	4,2

(This work is licensed under a Creative Commons Attribution 4.0 International License.)

International Journal of Engineering Research & Technology (IJERT)
ISSN: 2278-0181
Volume 13, Issue 01 January 2024

TABLE XXXVII. PREDICTING NPSHR FOR REF.[30] EXPERIMENT

Q/Q_{BE}	Experiment	Prediction
0,67	1,9	2,12
1	2,65	2,86
1,3	3,44	3,59
1,49	4,1	4,29

TABLE XXXVIII. PREDICTING NPSHR FOR REF.[31] EXPERIMENT

Q/Q_{BE}	Experiment	Prediction
0,6	2	2,09
0,8	2,7	2,79
1	3,4	3,49
1,2	4,1	4,19

TABLE XXXIX. PREDICTING NPSHR FOR REF.[32] EXPERIMENT

Q/Q_{BE}	Experiment	Prediction
0,8	2	2,16
0,92	2,63	2,83
1	3,3	3,49
1,05	3,94	4,14

TABLE XL. PREDICTING NPSHR FOR REF.[33] EXPERIMENT

Q/Q_{BE}	Experiment	Prediction
0,8	2,4	2,16
0,9	3,05	2,83
1	3,7	3,49
1,1	4,4	4,16

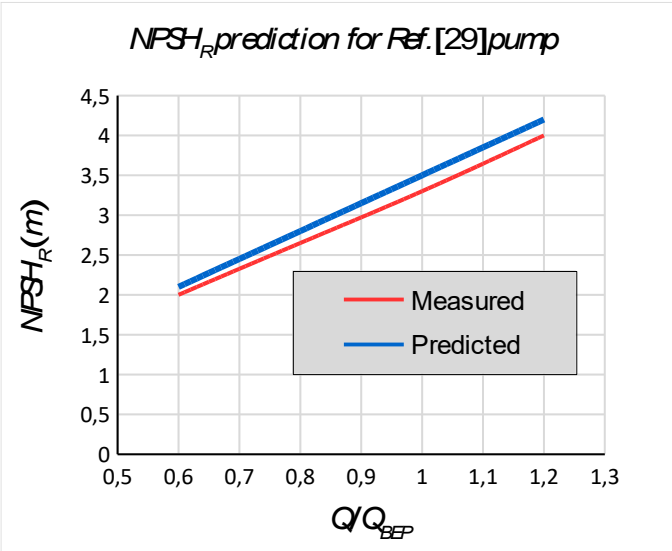

Fig. 3.19. Predicting $NPSH_R$ for [29] pump.

(This work is licensed under a Creative Commons Attribution 4.0 International License.)

International Journal of Engineering Research & Technology (IJERT)
ISSN: 2278-0181
Volume 13, Issue 01 January 2024

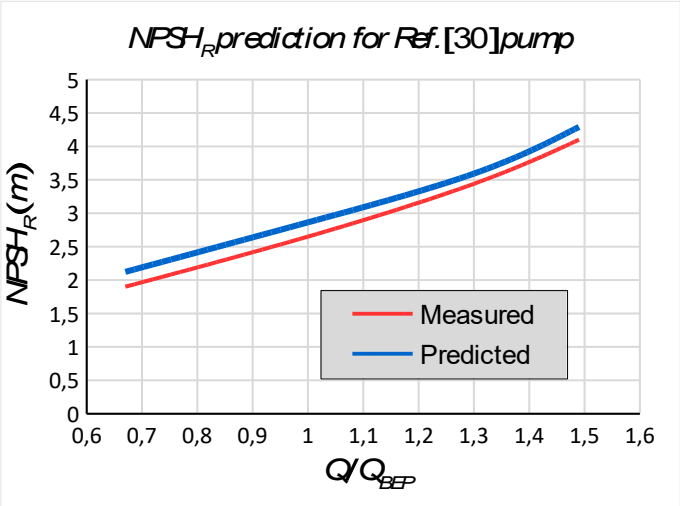

Fig. 3.20. Predicting $NPSH_R$ for [30] pump.

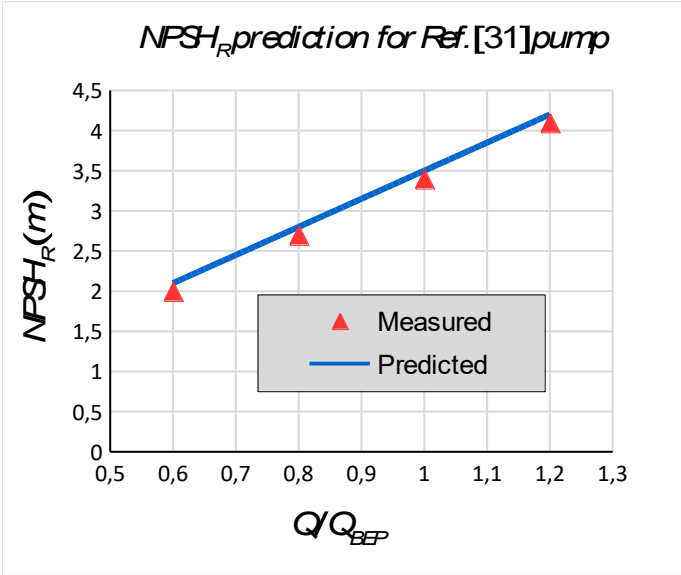

Fig. 3.21. Predicting $NPSH_R$ for [31] pump.

(This work is licensed under a Creative Commons Attribution 4.0 International License.)

International Journal of Engineering Research & Technology (IJERT)
ISSN: 2278-0181
Volume 13, Issue 01 January 2024

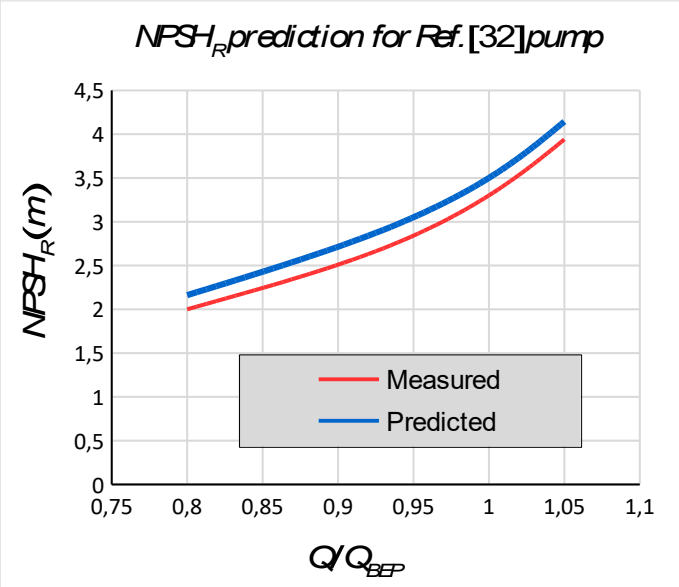

Fig. 3.22. Predicting $NPSH_R$ for [32] pump.

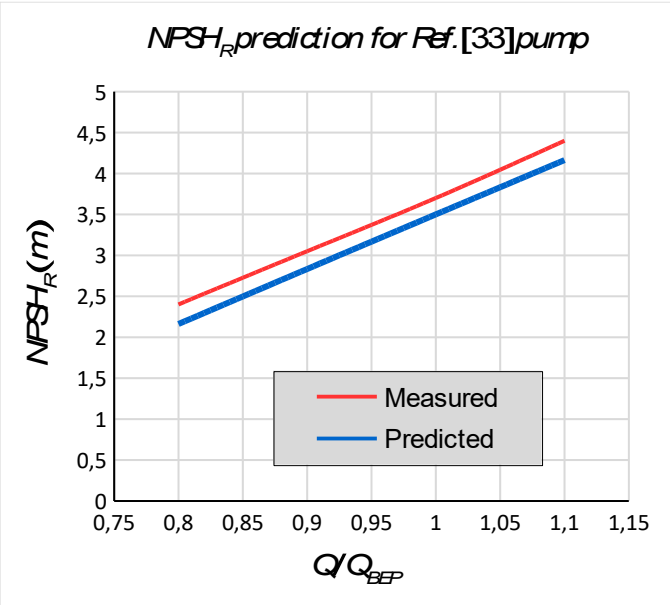

Fig. 3.23. Predicting $NPSH_R$ for [33] pump.

III. ESTIMATING PRESENT PUMP PERFORMANCE

As we said in the previous chapter, the best way to have accurate knowledge of the performance of the pump we designed would be to build it and then measure its performance in the test room. But this is quite difficult, costly and time-consuming. Alternatively we can make an estimate of the performances by making use of the empirical relationships we proposed in the previous chapter. This is what we attempt below in A and B.

A. Estimating present pump head

Eq.(2.8) gives: u_2=31 m/s.

(This work is licensed under a Creative Commons Attribution 4.0 International License.)

International Journal of Engineering Research & Technology (IJERT)
ISSN: 2278-0181
Volume 13, Issue 01 January 2024

By knowing that g=9.81 m/s^2, Eq. (3.2) gives:

$$H_{BEP} = 0.575\, u_2^2 / g = 0.575 \cdot 31_2^2 / 9.81 = 56.32\, m$$

Therefore, Eq.(3.1) finds:

$H_{shut\ off} = 1{,}17 \cdot H_{BEP} = 1{,}17 \cdot 56.32 = 65.9$ m

Eq.(2.6) gives: D_2=0.31 m.

Eq.(2.17) gives: b_2=0.024 m.

Therefore, Eq.(3.5) finds:

$$Q_{BEP} = 3600 \cdot (0.1 \cdot \pi \cdot u_2 \cdot b_2 \cdot D_2^{3.695})^{0.49} \rightarrow$$

$$Q_{BEP} = 3600 \cdot (0.1 \cdot 3.14 \cdot 31 \cdot 0.024 \cdot 0.31_2^{3.695})^{0.49} \rightarrow$$

$$Q_{BEP} = 211.86\, m^3/h$$

We can now calculate the pump head via equations (3.3a) until (3.3g). The results of the calculations are shown in the Table XLI where j is calculated according to Eq.(3.4):

$j = Q/Q_{BEP}$

In the Table XLI we have divided the interval 0-300 m^3/h into intervals of 50 m^3/h.

TABLE XLI. PRESENT PUMP HEAD PREDICTION

j	Q	Eq.(3.3a)	Eq.(3.3b)	Eq.(3.3c)	Eq.(3.3d)	Eq.(3.3e)	Eq.(3.3f)	Eq.(3.3g)
0	0	65,9	65,9	65,9	65,9	65,9	65,9	65,9
0,24	50	65,34	65,17	65,8	65,35	65,2	65,24	65,45
0,47	100	63,63	62,97	65,04	63,66	63,09	63,28	64,08
0,71	150	60,74	59,3	62,98	60,76	59,58	60,04	61,82
0,94	200	56,61	54,16	58,97	56,48	54,72	55,58	58,7
1,18	250	51,08	47,55	52,37	50,6	48,62	49,98	54,76
1,42	300	43,88	39,48	42,52	42,78	41,5	43,31	50,06

A graphical representation of the results of Table XLI is shown in Figure 4.1.

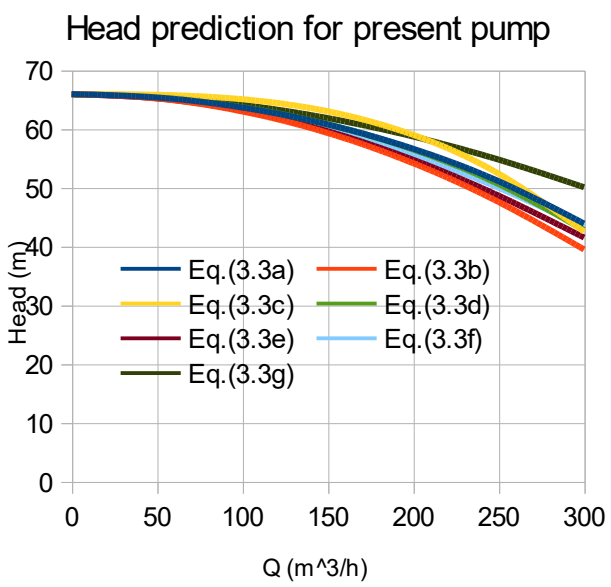

Fig. 4.1. Predicting head for present pump.

(This work is licensed under a Creative Commons Attribution 4.0 International License.)

International Journal of Engineering Research & Technology (IJERT)
ISSN: 2278-0181
Volume 13, Issue 01 January 2024

B. Estimating present pump efficiency

Now using η_{MAX}=0.8 [from Eq.(2.30)] and Equations 3.11 we can construct a Table similar to Table XLI for predicting pump efficiency. The results are shown numerically in Table XLII and graphically in Fig.4.2.j

TABLE XLII. Present Pump Efficiency Prediction

j	Q	Eq.(3.11a)	Eq.(3.11b)	Eq.(3.11c)	Eq.(3.11d)	Eq.(3.11e)	Eq.(3.11f)	Eq.(3.11g)
0	0	0	0	0	0	0	0	0
0,24	50	0,29	0,31	0,33	0,34	0,34	0,35	0,33
0,47	100	0,54	0,57	0,58	0,59	0,58	0,58	0,58
0,71	150	0,72	0,74	0,73	0,74	0,73	0,73	0,73
0,94	200	0,8	0,81	0,8	0,77	0,8	0,8	0,8
1,18	250	0,77	0,77	0,77	0,72	0,77	0,77	0,77
1,42	300	0,64	0,64	0,66	0,63	0,67	0,67	0,66

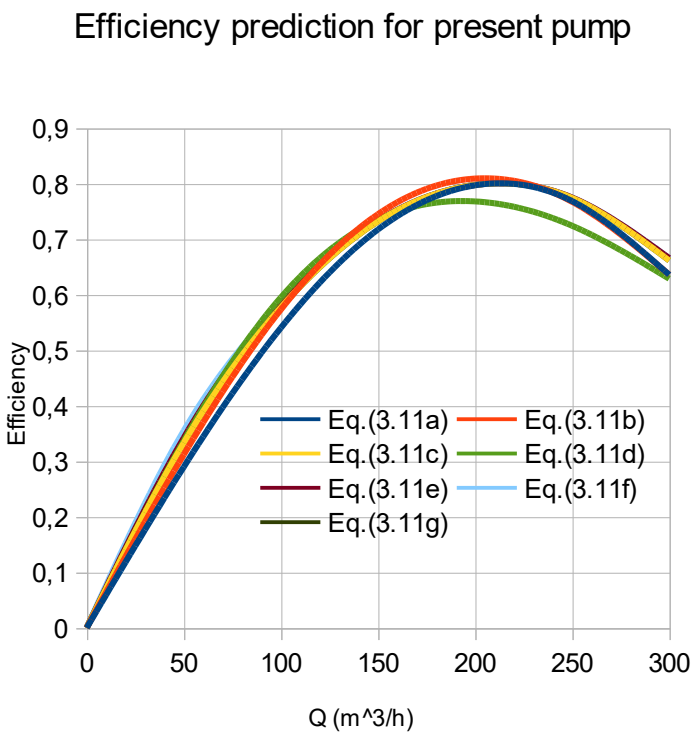

Fig. 4.2. Predicting efficiency for present pump.

IV. DISCUSSION OF RESULTS

Observing the comparison results in Chapter III, we can make the following findings:
The present model predicts the efficiency and manometric head curves quite well showing a slight underestimation for large dischargerates.
The prediction of $NPSH_R$ is equally satisfactory, showing however a systematic trend of slight overestimation in the majority of cases.

(This work is licensed under a Creative Commons Attribution 4.0 International License.)

International Journal of Engineering Research & Technology (IJERT)
ISSN: 2278-0181
Volume 13, Issue 01 January 2024

CONCLUSIONS

In the present study, a radial centrifugal pump was numerically investigated. Design models of impeller, volute, and combined impeller-diffuser geometry were developed. The impeller and diffuser geometry was developed in order to analyze the effects of the design parameters, including the blade shape, the blade height, the outlet blade angle, the blade width, the blade number, the impeller outer diameter and the overall efficiency. A good agreement was observed, when comparing the model numerical results with the experimental data obtained by a pump test rig.

Moreover, a group of empirical equations was developed in order to estimate the performance curves (H-Q, η–Q, $NPSH_R$-Q) of a centrifugal pump, using quite simple geometric data. The development of these equations prove that the prediction of centrifugal pumps performance curves could be accomplished without using complex mathematical models.

Furthermore, all-basic parameters that affect the pump behavior are taken into account resulting on very good approach to some original pump performance curves. The developed empirical formulas satisfactorily provide the ability to approximate the potential performance head, efficiency and cavitation curves of some commercial centrifugal pumps.

Nomenclature

English symbols		
A	section area	m^2
a_1	absolute flow angle	degrees
b	Blade section width	m
D	Impeller diameter	m
d	Shaft diameter	mm
g	gravitational acceleration	m/s^2
H	head	m
Q	discharge	m^3/h or m^3/s
M_s	shaft torque	N·m
N	power	Watts
n	rotational speed	rpm
n_q	specific speed	
r	impeller radius	m
u	peripheral (or tangential) velocity	m/s
$V_m = c_m$	meridional flow velocity	m/s
$V_u = c_u$	peripheral components of the absolute velocity	m/s
w	angular velocity of rotation	rad/s
z	Number of blades	
Greek symbols		
β	Blade angle	degrees
η	efficiency	
θ	temperature	Celcius degrees
ν	Kinematic viscosity	m^2/s
ρ	flow density	kg/m^3
φ	Wrap angle	degrees
Subscripts		
1	impeller inlet	
2	impeller outlet	
Abbreviations		

(This work is licensed under a Creative Commons Attribution 4.0 International License.)

International Journal of Engineering Research & Technology (IJERT)
ISSN: 2278-0181
Volume 13, Issue 01 January 2024

BEP	best efficiency point	
NPSH	Net Positive Suction Head	m

MEMORANDA

In memory of our professors and teachers in special education and science:
Prof. D. Papailiou, Department of mechanical engineering, University of Patras, Greece.
Prof. H.Marcinowski, Department of mechanical engineering, University of Karlsruhe,Germany.

REFERENCES

[1] K.Menny, "Stroemungsmaschinen", Teubner Verlag 1985.
[2] M.A., El-Naggar, "A One Dimensional Flow Analysis for the Prediction of Centrifugal Pump Performance Characteristics", International Journal of Rotating Machinery, Vol. 2013.
[3] J.F. Gülich, "Centrifugal Pumps", 2nd edition, Springer: Berlin,2010.
[4] H.Sigloch, "Stroemungsmaschinen" ,Hanser Verlag 1984.
[5] W. Bohl, "Strömungsmachinen 2", 5th edition, Vogel:Würzburg,1995.
[6] M. Teodor, "Impeller Design Using CAD Techniques and Conformal Mapping Method" Polytechnic University of Timisoara, Romania, 2012.
[7] V. A.Grapsas, J. S. Anagnostopoulos and D. E. Papantonis, "PARAMETRIC STUDY AND DESIGN OPTIMIZATION OF RADIAL FLOW PUMP IMPELLER", Laboratory of Hydraulic Turbomachines School of Mechanical Engineering / Fluids Section National Technical University of Athens, Greece.
[8] J.Kurokawa, "Simple formulae for volumetric efficiency and mechanical efficiency of hydraulic machinery", Conference on fluid machinery Osaka 1990. https://ynu.repo.nii.ac.jp/?action=repository_action_common_download&item_id=3858&item_no=1&attribute_id=22&file_no=1
[9] H. Li, H. Lin, W. Huang, J. Li, M. Zeng, J. Ma and X. Hu, "A New Prediction Method for the Complete Characteristic Curves of Centrifugal Pumps", Energies 2021, 14.
[10] X. Zhou, Y. Zhang, Z. Ji, and H. Hou, "The Optimal Hydraulic Design of Centrifugal Impeller Using Genetic Algorithm with BVF", Hindawi Publishing Corporation ,International Journal of Rotating Machinery Volume 2014.
[11] N. Athanassiadis, "Potential flow through spiral Casings", Dissertation 1961, ETH Zuerich.
[12] H. Zhang, L. Tang, and Y. Zhao, "Influence of Blade Profiles on Plastic Centrifugal Pump Performance", Hindawi ,Advances in Materials Science and Engineering ,Volume 2020,
[13] "Hydraulic design method for low specic speed overload free centrifugal pump impeller", google patent ,2014- 11-26 CN 201410712052 .
[14] J.C. Statharas, E. S. Valamontes, P. Filiousis and N. W. Vlachakis, "Strategies for Predicting Centrifugal Pump Performance Characteristics by Validating Blade Shape Configurations. Introducing the Trojan Horse Method", International Journal of Engineering Research & Technology (IJERT), Vol. 8 Issue 06, June-2019
[15] J. F. Gólich, "Centrifugal Pumps", Springer Berlin Heidelberg New York 2007
[16] V.N. Vlachakis, "Turbulent characteristics in stirring vessels: a numerical investigation", Virginia Tech 2006.
[17] N. Vlachakis, "Vergleich zweier Geschwindigkeitansätze für diε radiale Spaltstroemung in Bezug auf das Drehmoment der Rotierenden Scheibe", Bericht Universitaet Karlsruhe 1974.
[18] H.Siegle, "Die Radialspaltstroemung fuer Fluessigkeiten mit grossen Prandtl-Zahlen und Temperaturahhaengiger Viskositaet", Dissertation Universitaet Karlsruhe 1974.
[19] L. Zhou, W. Shi, and S. Wu, "Performance Optimization in a Centrifugal Pump Impeller by Orthogonal Experiment and Numerical Simulation", Hindawi Publishing Corporation Advances in Mechanical Engineering Volume 2013.
[20] K. C. Thin, M. M. Khaing, and K. M. Aye, "Design and Performance Analysis of Centrifugal Pump", World Academy of Science, Engineering and Technology 46 2008.
[21] T. Lei, Z. Baoshan, C. Shuliang, B. Hao, and W. Yuming, "Influence of Blade Wrap Angle on Centrifugal Pump Performance by Numerical and Experimental Study". CHINESE JOURNAL OF MECHANICAL ENGINEERING Vol. 27, No. 1, 2014.
[22] A. K. Omar, A. Khaldi and A. Ladouani, "Prediction of centrifugal pump performance using energy loss analysis", Australian Journal of Mechanical Engineering 2017.
[23] W. Li, X. Jiang, Q. Pang, L. Zhou and W. Wang, "Numerical simulation and performance analysis of a four-stage centrifugal pump", Advances in Mechanical Engineering, 2016, Vol. 8(10) 1–8.
[24] X. Han, Y. Kang, D. Li and W. Zhao, "Impeller Optimized Design of the Centrifugal Pump: A Numerical and Experimental Investigation", *Energies* 2018.
[25] H. Wang, B. Long, C. Wang, C. Han and L. Li, "Effects of the Impeller Blade with a Slot Structure on the Centrifugal Pump Performance", Energies 2020.
[26] M. Djerroud, G. D. Ngoma, and W. Ghie, "Numerical Identification of Key Design Parameters Enhancing the Centrifugal Pump Performance: Impeller, Impeller-Volute and Impeller-Diffuser". International Scholarly Research Network ISRN Mechanical Engineering Volume 2011.
[27] J.-H. Kim, H.-C. Lee, J.-H. Kim, S. Kim, J.-Y. Yoon and Y.-S. Choi, "Design techniques to improve the performance of a centrifugal pump using CFD", Journal of Mechanical Science and Technology 29 (1) (2015).
[28] A. ALMASLAMANI, M. CONSTANTIN1, N. BARAN and M. M. STOICAN, "EXPERIMENTAL STUDY OF THE PERFORMANCE AND PREDICTION OF CAVITATION PHENOMENON FOR A VARIABLE SPEED CENTRIFUGAL PUMP", Journal of Science and Arts Year 20, No. 1(50), pp. 225-238, 2020.
[29] Md Rakibuzzaman, S.-H. Suh, H.-H. Kim and Y.-H. Jang, "Relationship between Cavitation Incipient and NPSH Characteristic for Inverter Drive Centrifugal Pumps", The KSFM Journal of Fluid Machinery: Vol. 18, No. 6, December, 2015.
[30] B. Schiavello and F.C.Visser, "Pump cavitation", Pump symposium 2009.
[31] J. Pei, M. K. Osman, W. Wang, D. Appiah, T. Yin and Q. Deng, "A Practical Method for Speeding up the Cavitation Prediction in an Industrial Double-Suction Centrifugal Pump", Energies 2019, 12.
[32] R. Kliem, "Experimentelle und numerische Untersuchung zum Einfluss von Einbaubedingungen auf das Betriebs- und Kavitationsverhalten von Kreiselpumpen", Dissertation 2006, Technische Universität Darmstadt.
[33] M. Kaya and E. Ayder, "Prediction of Cavitation Performance of Radial Flow Pumps", *Journal of Applied Fluid Mechanics*, Vol. 10, No. 5, pp. 1397-1408, 2017.

(This work is licensed under a Creative Commons Attribution 4.0 International License.)